NASA
Reference
Publication
1131

September 1984

Engineering and Design Properties of Thallium-Doped Sodium Iodide and Selected Properties of Sodium-Doped Cesium Iodide

K. Forrest, C. Haehner,
T. Heslin, M. Magida,
J. Uber, S. Freiman,
G. Hicho, and R. Polvani

NASA

NASA
Reference
Publication
1131

1984

Engineering and Design Properties of Thallium-Doped Sodium Iodide and Selected Properties of Sodium-Doped Cesium Iodide

K. Forrest, C. Haehner,
T. Heslin, M. Magida,
and J. Uber
Goddard Space Flight Center
Greenbelt, Maryland

S. Freiman, G. Hicho,
and R. Polvani
National Bureau of Standards
Washington, D.C.

NASA
National Aeronautics
and Space Administration

Scientific and Technical
Information Branch

All measurement values are expressed in the International System of Units (SI) in accordance with NASA Policy Directive 2220.4, paragraph 4.

CONTENTS

ENGINEERING AND DESIGN PROPERTIES OF THALLIUM-DOPED SODIUM IODIDE AND SELECTED PROPERTIES OF SODIUM-DOPED CESIUM IODIDE

K. Forrest, C. Haehner, T. Heslin, M. Magida, J. Uber
NASA/Goddard Space Flight Center
Greenbelt, Maryland 20771

S. Freiman, G. Hicho, R. Polvani
National Bureau of Standards
Washington, D.C. 20234

INTRODUCTION

The experiments selected for the Gamma Ray Observatory (GRO) will utilize over 1000 kg of inorganic NaI(Tl) and CsI(Na) scintillators. Many of the individual blocks of scintillators will be larger than any that have previously been launched in a space vehicle. The Energetic Gamma Ray Experiment (EGRET) scintillator, for example, is a composite assembly of NaI(Tl) approximately 0.76 m square by 20 cm thick, and the Oriented Scintillation Spectrometer Experiment (OSSE) uses a 0.33 m diameter cylinder composed of a 10 cm thick piece of NaI(Tl) and a 7.6 cm thick piece of CsI(Na). Proper mechanical systems design for the encapsulation, bonding, and support of these large scintillator blocks is necessary if performance degradation from cracking near support regions or failure because of creep or clouding from hydration are to be avoided. On the other hand, overdesigned support systems that result in large weight penalties are also to be avoided.

Although the alkali halides have been studied for years, most of the work in the 1950's and 1960's centered on NaCI, KCI, LiF, and cubic materials such as MgO because these materials were model systems for delineating solid-state theories about defect structures that were the subject of extensive research at the time. Other than some work on CsI done for the High Energy Astronomy Observatory in the early 1970's (references 1 and 2), the only engineering properties study of NaI was a report of limited circulation by Stanford University (reference 3) and undoped, single-crystal elastic constant data in Landolt-Bornstein (reference 4).

To optimize the mechanical design of the scintillator supports and housings for experiments, the GRO systems team authorized a program for determining accurate and statistically significant values for the mechanical and thermal properties of NaI(Tl) and selected properties of CsI(Na). The

ensuing materials evaluation program was conducted by the Materials Control and Applications Branch of the Goddard Space Flight Center (GSFC) and the Fracture and Deformation Division of the National Bureau of Standards under contract to GSFC. Emphasis of the program was placed on the needs of the EGRET and OSSE programs. This test report was compiled from the results of this test program. In addition, other test results and literature data that were not developed in this program are cited to make this compilation as comprehensive as possible for those who wish to use these two materials in mechanical designs. Enough test description and analysis of the data is presented to facilitate comparative testing in the future.

In the following section, a series of ten test requirements are outlined, beginning with coefficient of linear thermal expansion and ending with ingot variation of strength. This sequence of properties is the topic outline for each succeeding section in this report, beginning with summary of results and ending with the conclusions.

TEST REQUIREMENTS

The following properties of single-crystal and polycrystalline NaI(Tl) were required for meeting the needs of the various GRO experiments:

1. Coefficient of linear thermal expansion
2. Thermal conductivity
3. Thermal-shock resistance
4. Heat capacity
5. Elastic constants
    a. Density
    b. Young's modulus
    c. Shear modulus
    d. Mechanical damping efficiency (internal friction)
6. Ultimate strengths
    a. Modulus of rupture
    b. Shear
    c. Compressive
    d. Critical stress intensity factor (K_{IC})
7. Creep
    a. Bending
    b. Compression

8. Hardness
9. Susceptibility to subcritical crack growth
10. Ingot variation of strength

In addition, it was determined that compressive strength and compressive creep measurements were necessary for single-crystal CsI(Na).

Material for all tests was purchased from the Harshaw Chemical Company, Solon, Ohio, and the Bicron Corporation, Newbury, Ohio.

SUMMARY OF RESULTS

This section summarizes the test results for single-crystal and polycrystalline NaI(Tl) and single-crystal CsI(Na). After each property heading, the symbol subsequently used to refer to the property is listed, and the range of values measured for that property is given without regard to the values referring to single-crystal or polycrystalline material unless otherwise stated.

Finally, an evaluated average, plus or minus one standard deviation, is given when applicable along with the number (n) of data points used to arrive at the standard deviation. The evaluated average is arrived at in the section entitled "Test Results and Statistical Analysis" and usually represents the average of the largest group of specimens that cannot be statistically differentiated from each other using a pair-wise t-test of the equality of means at the 90- or 95-percent confidence level. In the short text after each heading, some details on the effects of orientation and position are given for single-crystal and Polyscin* materials, and the effects of ingot variation are cited. An abbreviation key referring to position and orientation designations for Polyscin and single-crystal material appears in Table 4.

Coefficient of Linear Thermal Expansion, α

- Range 45.65×10^{-6} K^{-1} to 50.20×10^{-6} K^{-1} at 253 to 323 K
- Evaluated average $(47.21 \pm 0.44) \times 10^{-6}$ K^{-1} at 297 to 323 K, n = 9

Measurements were made on three oriented single-crystal and four Polyscin NaI(Tl) specimens. Single-crystal material exhibited the same coefficient of linear thermal expansion in the <100>, <011>, and <111> directions. The coefficient of linear thermal expansion of Polyscin is slightly less in the direction perpendicular to the extrusion axis than in the direction parallel to it, and there is no significant difference between similarly positioned material taken from the beginning or end of an extrusion.

Literature values are as follows:

- Single-crystal, undoped NaI 44.7×10^{-6} K^{-1}, 293 K (reference 5, page 1116)
- Single-crystal, undoped CsI 48.3×10^{-6} K^{-1}, 293 K (reference 5, page 1098)

*"Polyscin" is a polycrystalline form of NaI(Tl) produced by the Harshaw Chemical Company.

Thermal Conductivity, k

- Range 1.47×10^{-2} to 1.91×10^{-2} W/cm K at 300 K
- Evaluated average $(1.71 \pm 0.28) \times 10^{-2}$ W/cm K at 300 K, n = 43

Measurements were made on three oriented single-crystal NaI(Tl) specimens and four Polyscin specimens. Single-crystal material exhibited the same thermal conductivity in the <100> and <011> directions, but exhibited a lower value in the <111> direction. Polyscin material from the interior of the initial end of an extrusion exhibited the highest measured thermal conductivity in the direction parallel to the extrusion axis. Measurements made on the other three Polyscin specimens and the <100> and the <011> single-crystal specimens were statistically indistinguishable at the 90-percent confidence level.

Literature values are as follows:

- Single crystal, undoped NaI, 1.53×10^{-2} W/cm K at 300 K (reference 3, page 2)
- Single crystal, undoped CsI, 1.05×10^{-2} W/cm K at 296 K (reference 6, page 561)

Thermal Shock Resistance, ΔT_c

In oil-quench tests of 23 NaI(Tl) specimens, ΔT_c ranged from 18.5 to 33.5 K for material with a surface area to volume ratio of 1.83 and 3.4 cm^{-1}, respectively. In air-quench tests of four NaI(Tl) specimens, ΔT_c ranged from 59.5 to 67 K for material with a surface area to volume ratio of 1.83 cm^{-1} and 3.4 cm^{-1}, respectively.

Analysis indicates that, for initial crack sizes in the range of 2.5 mm (which was average in the Polyscin examined), ΔT_c ranges from a low of 3.3 K for a very high heat-transfer coefficient and Biot modulus ($h \rightarrow \infty$, $\beta >> 100$) to a high of about 25 K for oil quenching ($h^* = 0.037$ W/cm^2 K, $\beta^* = 0.628$) and 67 K for air quenching ($h^* = 0.012$ W/cm^2 K, $\beta^* = 0.23$).

Heat Capacity, C_p

- Range 0.346 to 0.350 J/gK at 310 K
- Evaluated average $0.348 \pm 6.61 \times 10^{-3}$ J/gK, at 310 K, n = 28

Four NaI(Tl) specimens were measured; two single-crystal and two Polyscin specimens. No significant difference was observed between the specimens.

Literature values are as follows:

- NaI (undoped) 0.347 J/gK at 273 K
  0.355 J/gK at 323 K (reference 7, page 2273)
- CsI (undoped) 0.203 J/gK at 298 K (reference 8, page 496)

*Calculated values.

Elastic Constants, ρ, E, G, C_{ij}, Q^{-1}, all at 300 K

ρ – range 3.657 to 3.675 g/cc
evaluated average 3.67 ± 5.61 X 10^{-3} g/cc, n = 35

E – range 1.9129 X 10^4 MPa ($E_{<111>}$) to 2.6263 X 10^4 MPa ($E_{<100>}$)
evaluated average 2.01508 X 10^4 MPa ± 0.06258 X 10^4 MPa (Polyscin), n = 50

G – range 7.35 X 10^3 MPa ($G_{<100><010>}$) to 1.07 X 10^4 MPa ($G_{<011><0\bar{1}1>}$)
evaluated average 7.6470 X 10^3 MPa ± 0.2857 X 10^3 MPa (Polyscin), n = 50

C_{11} – range 3.0250 to 3.0747 X 10^4 MPa
evaluated average 3.0418 X 10^4 ± 0.0117 X 10^4 MPa, n = 36

C_{12} – range 8.7790 to 9.1125 X 10^3 MPa
evaluated average 8.9581 X 10^3 ± 0.1035 X 10^3 MPa, n = 36

C_{44} – range 7.3305 to 7.4368 X 10^3 MPa
evaluated average 7.3601 X 10^3 ± 0.0262 X 10^3 MPa, n = 36

Q^{-1} – range 2.80 X 10^{-4} to 5.30 X 10^{-4} at 750 Hz
evaluated average 5.12 X 10^{-4} ± 1.3 X 10^{-4}, n = 8

The average value for Young's, shear, and bulk moduli for Polyscin are 2.01 X 10^4, 7.64 X 10^3, and 1.80 X 10^4 MPa, respectively, and Poisson's ratio is 0.314, there being a 4.2 to 7.3-percent difference in the value of these constants corresponding to the degree that the material has been work-hardened in the forming operation. Material tested from two separate logs of Polyscin had the same elastic constants, ρ, E, and G. Material from two different single-crystal ingots had the same elastic constants, ρ and C_{ij}.

Literature values are as follows:

- NaI at 300 K
  - ρ = 3.667 g/cc (reference 7, page 656)
  - E = 2.08 X 10^4 MPa (Polyscin) (reference 3, page 1)
  - G = 7.86 X 10^3 MPa (Polyscin) (reference 3, page 1)
  - C_{11} = 3.03 X 10^4 MPa (reference 4, page 8)
  - C_{12} = 8.9 X 10^3 MPa (reference 4, page 8)
  - C_{44} = 7.34 X 10^3 MPa (reference 4, page 8)
- CsI at 300 K
  - ρ = 4.510 g/cc (reference 7, page 656)
  - E = 1.39 X 10^4 MPa (Polycrystal) (reference 2, page 4)
  - G = 6.9 X 10^3 MPa (Polycrystal) (reference 2, page 4)

C_{11} = 2.45×10^4 MPa (reference 4, page 8)

C_{12} = 6.7×10^3 MPa (reference 4, page 8)

C_{44} = 6.3×10^3 MPa (reference 4, page 8)

Ultimate Strength

NaI(Tl) at 300 K

- Modulus of rupture (MOR)

  <100> cleavage, range = 1.57 to 2.71 MPa
  Polyscin, range = 2.85 to 6.49 MPa

- Shear

  <100> cleavage, range = 6.42 to 9.74 MPa
  Polyscin, range = 5.71 to 8.00 MPa

- Compression

  <100> cleavage, range = 11.19 to 16.72 MPa
  Polyscin, range = 9.11 to 23.12 MPa

- K_{IC}

  Polyscin, range = 0.304 to 0.436 MPa $m^{1/2}$
  Evaluated average = 0.382 ± 0.042 MPa $m^{1/2}$, n = 9

Material from two separate logs of Polyscin and nine different NaI(Tl) single-crystal ingots was tested. Although Polyscin is homogeneous with respect to elastic moduli, its MOR strength in one extrusion varied significantly (a factor of 1.4 on average) with position in the log, whereas in the second extrusion, MOR strength was homogeneous. Single-crystal strengths are ingot-dependent within the ranges cited.

CsI(Na) at 300 K (0.2-percent yield)

- <100> single crystal, range = 3.27 to 7.49 MPa
- Polycrystal, average = 2.98 ± 0.22 MPa, n = 5

Material from three single-crystal ingots and one polycrystal ingot of CsI(Na) was tested. Yield strength varied extensively from ingot to ingot (as much as a factor of 2.3), but strength within an ingot was homogeneous.

Literature values are as follows:

- NaI(Tl)

  MOR = 6.45 MPa (reference 3, Part 2, page 1)

- CsI(Na)

  Proportional limit = 0.276 to 2.35 MPa (reference 2, page 14)
  K_{IC} = 0.279 to 1.206 MPa $m^{1/2}$, single crystals*

Creep

NaI(Tl) at 300 K

- Compression

  Less than 0.005 percent in 2000 hours at 1.38 MPa (Polyscin)
  Less than 0.017 percent in 3000 hours at 1.08 MPa (<100> single crystal)

- Bending (four point)

  12.7- by 2.54- by 2.54-cm specimens, 10.6-cm outerspan, 3.386-cm inner span
  Less than 5.08×10^{-5} cm in 4000 hours at 1.93 MPa (Polyscin)
  Less than 7.62×10^{-4} cm in 4000 hours at 1.48 MPa (<100> single crystal)

Compressive and flexural creep in NaI(Tl) at 300 K can be expressed linearly using a $t^{1/3}$ plot, where t is time. An indication of creep rate is measured in terms of the slope of such a linear plot. An increasing slope indicates an increasing creep rate. Significant creep is considered to be the point of maximum rate of change in a plot of slope versus applied stress (Figure 19).

Material from one extrusion of Polyscin was tested in flexure and in compression. Material from one single crystal was tested in compression while material from another single crystal was tested in flexure.

In general, single-crystal material crept more than Polyscin for the same test. Compressive and flexural creep was greatest for single-crystal material stressed in a principal-axis, <100> direction, compared to material stressed in the other symmetry-axis directions, <011> and <111>.

For Polyscin, compressive creep is very small (<0.005 percent in 2000 hours) at stresses below 1.38 MPa. Material from the end of an extrusion, near the surface, creeps less than material from the interior of an extrusion near the beginning by a factor of about 0.72. This is attributed to a difference in the degree of work-hardening in these two regions.

In either case, relatively large creep rates (slope >10 microstrain/$hr^{1/3}$) do not occur until the proportional limit of the material is exceeded, which is, on the average, 2.43 MPa for interior material and 3.44 MPa for surface material. Maximum compressive creep was measured in a single crystal loaded in a principal-axis <100> direction. A strain of 0.135 percent was measured in 350 hours at 2.89 MPa.

*D. Lewis, Personal Communication, Ceramics Branch, Naval Research Laboratory, Washington, D.C.

In flexure, creep in Polyscin begins when the maximum flexural stress exceeds 1.93 MPa. Below this stress level, no observable creep was detected in 4000 hours with a sensitivity of 5.08×10^{-5} cm. In contrast with compressive creep, flexural creep in Polyscin is homogeneous with respect to position and orientation in an extrusion. Relatively large creep rates (slope $>5.08 \times 10^{-6}$ cm/hr$^{1/3}$) do not occur until the proportional limit of the material is exceeded, which is, on the average, 3.03 MPa. Maximum flexural creep was measured in a single crystal loaded in a principal-axis <100> direction. A displacement of 7.62×10^{-4} cm was measured after 4000 hours at 1.72 MPa.

CsI(Na) at 300 K (Compression)

- Less than 0.858 percent in 979 hours at 2.25 MPa (polycrystal)
- Less than 0.139 percent in 1126 hours at 2.69 MPa (<100> single crystal)

The dominant feature of creep behavior of the CsI(Na) is the high variability between crystal ingots.

Vickers Hardness, H

- Range 7.74 to 9.5 kg/mm^2 (single crystal)
- Evaluated average 8.12 ± 0.6 kg/mm^2

The hardness of single-crystal NaI(Tl) is independent of crystallographic direction.

Susceptibility to Subcritical Crack Growth

Stress-rate tests indicate that Polyscin NaI(Tl) is not susceptible to subcritical crack growth in the stress-rate range from 0.132 to 63.8 MPa/second. Plastic deformation behavior is observed in this stress-rate range. At higher rates, in excess of 1.4×10^4 MPa/second, strength increased relative to the values exhibited at the lower stress rates by a factor of 2 to 5 times, and brittle fracture was observed.

Ingot Variation of Strength

NaI(Tl)

A study of the MOR, <100> single-crystal cleavage strength of 38 NaI(Tl) specimens from eight different ingots indicates that strength is ingot-dependent but homogeneous within an ingot. Average strengths varied from 1.75 to 2.58 MPa.

A similar study of the MOR strengths of 24 specimens from one extrusion of Polyscin and eight specimens from another extrusion indicated that the second extrusion was homogeneous with respect to strength, whereas the first one was not. Average MOR strength is extrusion-dependent, and varied from 4.03 to 5.6 MPa. The thallium concentration in NaI(Tl) was measured for each of the MOR test specimens. No correlation was found to establish a strength dependency on the basis of thallium concentration.

A compressive initial cracking-strength (ICS) study of eight Polyscin specimens from both of two extrusions indicates that ICS is ingot-dependent and is not homogeneous within an ingot. Average strengths varied from 11.4 to 18.9 MPa.

CsI(Na)

A study of the 0.2-percent <100> compressive yield strength of nine single-crystal CsI(Na) specimens from three different ingots indicates that strength is ingot-dependent but homogeneous within an ingot. Average strengths varied from 3.50 to 7.36 MPa.

MATERIALS, SPECIMENS, AND TEST METHODS

Testing was divided into two general areas. NaI(Tl) testing was performed by GSFC, except for stress-rate testing and initial K_{IC} testing, which was addressed by the National Bureau of Standards (NBS). CsI(Na) testing was performed by NBS. Three separate specimen orders were received. GSFC received two orders of NaI(Tl) about 2 years apart (1980 and 1982), and NBS received one order of CsI(Na) and Polyscin NaI(Tl) in 1980. The Polyscin NaI(Tl) material in the NBS order was taken from a different extrusion than that of the material in the GSFC order; therefore, including the three specimens (two bonded and one solid) tested by Stanford University in 1976 (reference 3), four Polyscin extrusions have been sampled and documented. The strength-test results for specimens from these four extrusions are summarized and discussed further in the section on "Test Results and Statistical Analysis."

The first order received by GSFC consisted of 144 NaI(Tl) specimens from the Harshaw Chemical Company and 51 specimens from the Bicron Corporation.

One extrusion of Polyscin and three ingots of single-crystal material were represented in this order. The second GSFC order consisted of 16 Polyscin and 24 single-crystal ultimate-strength specimens, representing one polycrystalline extrusion and six single-crystal ingots. Including the first order of material, nine single-crystal ingots have been sampled and documented. Strength-test results of specimens from these nine ingots are summarized and discussed further in the section on "Test Results and Statistical Analysis."

The NaI(Tl) portion of the NBS order consisted of 68 Polyscin MOR specimens for stress-rate testing and six double-cantilever beam specimens for K_{IC} measurements. The CsI(Na) portion of the NBS order consisted of 15 single-crystal compression specimens and five polycrystalline specimens. The 15 single-crystal specimens represented three different ingots and the three symmetry-axis directions, as well as top, middle, and bottom positions in an ingot (reference 9).

Specimens for corroborative K_{IC} testing (measurement No. 6d) hardness (No. 8) and impact testing (No. 9) were made and tested at GSFC from unused creep specimens or broken MOR bars.

Tables 1, 2, and 3 list the specimens. Table 4 identifies the symbols used in Tables 1, 2, and 3.

Table 1
GSFC Purchase No. 1 (1980)

Property	Test Number	Material Type*	Position*	Orientation*	Specimen Size (cm)	Number of Specimens
Coefficient of Linear Thermal Expansion	1	P	IH	//	5.08 X 0.555 dia	1
		P	IS	⊥	5.08 X 0.555 dia	1
		P	FH	//	5.08 X 0.555 dia	1
		P	FS	⊥	5.08 X 0.555 dia	1
		S,H	Any	<100>	5.08 X 0.555 dia	1
		S,H	Any	<011>	5.08 X 0.555 dia	1
		S,H	Any	<111>	5.08 X 0.555 dia	1
Thermal Conductivity	2	P	IH	//	0.954 X 5.08 dia	1
		P	IS	⊥	0.954 X 5.08 dia	1
		P	FH	//	0.954 X 5.08 dia	1
		P	FS	⊥	0.954 X 5.08 dia	1
		S,B	Any	<100>	0.954 X 5.08 dia	1
		S,B	Any	<011>	0.954 X 5.08 dia	1
		S,B	Any	<111>	0.954 X 5.08 dia	1
Specific Heat	3	P	IH	Any	0.635 dia X 0.127	1
		P	FS	Any	0.635 dia X 0.127	1
		S,H	Any	Any	0.635 dia X 0.127	1
Thermal Shock Resistance	4	P	FS	//	2.54 X 7.62 X 7.62	3
		P	IH	⊥	2.54 X 7.62 X 7.62	3
		S,B	Any	<100>	2.54 X 7.62 X 7.62	3
Elastic Moduli and Damping	5	P	IH	//	12.7 X 2.54 X 0.475	2
		P	IH	⊥	12.7 X 2.54 X 0.475	2
		P	IS	//	12.7 X 2.54 X 0.475	2
		P	FH	//	12.7 X 2.54 X 0.475	2
		P	FH	⊥	12.7 X 2.54 X 0.475	2
		P	FS	//	12.7 X 2.54 X 0.475	2
		S,H	Any	<100>	12.7 X 2.54 X 0.475	2
		S,H	Any	<011>	12.7 X 2.54 X 0.475	2
		S,H	Any	<111>	12.7 X 2.54 X 0.475	2
Ultimate Bending Strength (4 point)	6a	P	IH	//	12.7 X 2.54 X 2.54	4
		P	IH	⊥	12.7 X 2.54 X 2.54	4
		P	IS	//	12.7 X 2.54 X 2.54	4
		P	FH	//	12.7 X 2.54 X 2.54	4
		P	FH	⊥	12.7 X 2.54 X 2.54	4
		P	FS	//	12.7 X 2.54 X 2.54	4
		S,H,& B	Any	<100>	12.7 X 2.54 X 2.54	3
		S,H,& B	Any	<011>	12.7 X 2.54 X 2.54	3
		S,H,& B	Any	<111>	12.7 X 2.54 X 2.54	3

*Table 4 defines symbols that appear in this table.

Table 1 (Continued)

Property	Test Number	Material Type*	Position*	Orientation*	Specimen Size (cm)	Number of Specimens
Ultimate Shear Strength	6b	P	FS	//	7.62 X 1.27 dia	4
		P	IH	⊥	7.62 X 1.27 dia	4
		S,H,& B	Any	<100>	7.62 X 1.27 dia	3
		S,H,& B	Any	<011>	7.62 X 1.27 dia	3
		S,H,& B	Any	<111>	7.62 X 1.27 dia	3
Ultimate Compression Strength	6c	P	FS	//	2.86 X 2.54 dia	4
		P	IH	⊥	2.86 X 2.54 dia	4
		S,H,& B	Any	<100>	2.86 X 2.54 dia	3
		S,H,& B	Any	<011>	2.86 X 2.54 dia	3
		S,H,& B	Any	<111>	2.86 X 2.54 dia	3
Bending Creep (4 point)	7a	P	FS	//	12.7 X 1.90 X 1.90	6
		P	IH	⊥	12.7 X 1.90 X 1.90	6
		S,B	Any	<100>	12.7 X 1.90 X 1.90	2
		S,B	Any	<011>	12.7 X 1.90 X 1.90	2
		S,B	Any	<111>	12.7 X 1.90 X 1.90	2
Compression Creep	7b	P	FS	//	2.54 X 0.635 dia	6
		P	IH	⊥	2.54 X 0.635 dia	6
		S,B	Any	<100>	2.54 X 0.635 dia	2
		S,B	Any	<011>	2.54 X 0.635 dia	2
		S,B	Any	<111>	2.54 X 0.635 dia	2

* Table 4 defines symbols that appear in this table.

Table 2
GSFC Purchase No. 2 (1982)

Property	Test Number	Material Type*	Position*	Orientation*	Specimen Size (cm)	Number of Specimens
Ultimate Compression	6c	P	IH	⊥	2.86 X 2.54 dia	4
		P	FS	//	2.86 X 2.54 dia	4
Ultimate Bending	6a	P	IH	//	12.7 X 2.54 X 2.54	4
		P	FH	//	12.7 X 2.54 X 2.54	4
		S,H	Any	<100>	12.7 X 2.54 X 2.54	24**

*Table 4 defines symbols that appear in this table.
**Four specimens from each of six different ingots.

Table 3
NBS Purchase (1980)

Property	Test Number	Material Type*	Position*	Orientation*	Specimen Size (cm)	Number of Specimens
Ultimate Bending (3 point) Stress-Rate Testing	6a	P	Any	Any	2.5 X 0.6 X 0.3	68
Double Cantilever Beam, K_{IC}	6d	P	Any	Any	5.0 X 1.9 X 0.2	6
0.2% Compression Yield and Creep	7b	C	S T M B B B	R <100> <100> <100> <110> <111>	1.27 X 0.635 dia 1.27 X 0.635 dia 1.27 X 0.635 dia 1.27 X 0.635 dia 1.27 X 0.635 dia 1.27 X 0.635 dia	5 3** 3** 3** 3** 3**

*Table 4 defines symbols that appear in this table.
**One specimen from each of three different ingots.

For <100>, <011>, and <111> specimens, the mutually perpendicular direction pairs <010>, <001>; <0$\bar{1}$1>, <100>; and <1$\bar{1}$0>, <$\bar{1}\bar{1}$2>, respectively, were indicated on the specimen, and for parallelepiped specimens, these directions were perpendicular to prismatic faces. The 12.7- by 2.54-cm faces of the elastic moduli and Q^{-1} specimens (property No. 5) were perpendicular to the <0$\bar{1}$1> direction for <011> specimens and perpendicular to the <$\bar{1}\bar{1}$2> direction for <111> specimens.

Specimens were received from the manufacturers in sealed cans. The cans were opened, and the specimens were inspected in an N_2 gas-purged glove box. The specimens were subsequently inventoried, stored in a bank of file drawers inside the dry glove box, and purged with the dry N_2 boiloff from an LN_2 tank as shown in Figure 1. The dryness of the purged gas was periodically measured with a hygrometer (Great Eastern Model 500) and was consistently found to be below a dew point of 253 K.

CsI(Na) specimens were also kept in a dry glove-box facility at the National Bureau of Standards similar to the one shown in Figure 1; however, precautions to maintain the low humidity necessary for testing NaI(Tl) were not necessary for CsI(Na). These specimens were tested in a laboratory environment (<50-percent relative humidity at 295 K).

NaI(Tl) specimens were kept dry and were isolated from ambient humidity at all times. They were transported, from dry storage boxes through air locks to the testing facility, in sealed containers filled with anhydrous $CaSO_4$.

Table 4
Symbols Key for Tables 1, 2, and 3

Symbol	Definition
Material Type Key	
P	NaI (Tl) Polyscin
S	NaI (Tl) single crystal
C	CsI (Na)
H	Harshaw Chemical Company material
B	Bicron Corporation material
Position Key	
I	Initial end of extrusion
F	Final end of extrusion
H	Heart of extrusion
S	Surface of extrusion
T	Top portion of a single-crystal ingot
M	Middle portion of a single-crystal ingot
B	Bottom portion of a single-crystal ingot
Orientation Key	
//	First dimension parallel to extrusion direction
⊥	First dimension perpendicular to extrusion direction
<100>	First dimension parallel to a Miller index <100> crystallographic direction
<011>	First dimension parallel to a Miller index <011> crystallographic direction
<111>	First dimension parallel to a Miller index <111> crystallographic direction
R	Random (orientation unknown)

Three methods of humidity reduction were necessary for maintaining moisture levels below a dew-point of 253 K, depending on the size of the enclosure. Small enclosures were continuously purged with dry N_2 from LN_2 tanks or compressed-gas bottles. Larger enclosures maintained a dry N_2 purge coupled with open containers of anhydrous $CaSO_4$. Because of the size of the creep facility, however, it was necessary to install a drying train to maintain sufficiently low humidity levels. In some cases, polished scrap pieces of NaI(Tl) were used as a visual moisture indicator; cloudiness indicates unacceptably high moisture levels.

Coefficient of Linear Thermal Expansion

Measurements were made according to ASTM E228-71 with a Custom Scientific Instruments Company model CS-128, quartz push-rod dilatometer. A National Bureau of Standards copper standard reference specimen was used to calibrate the instrument. The smallest displacement measurable with the apparatus was 7.62×10^{-5} cm.

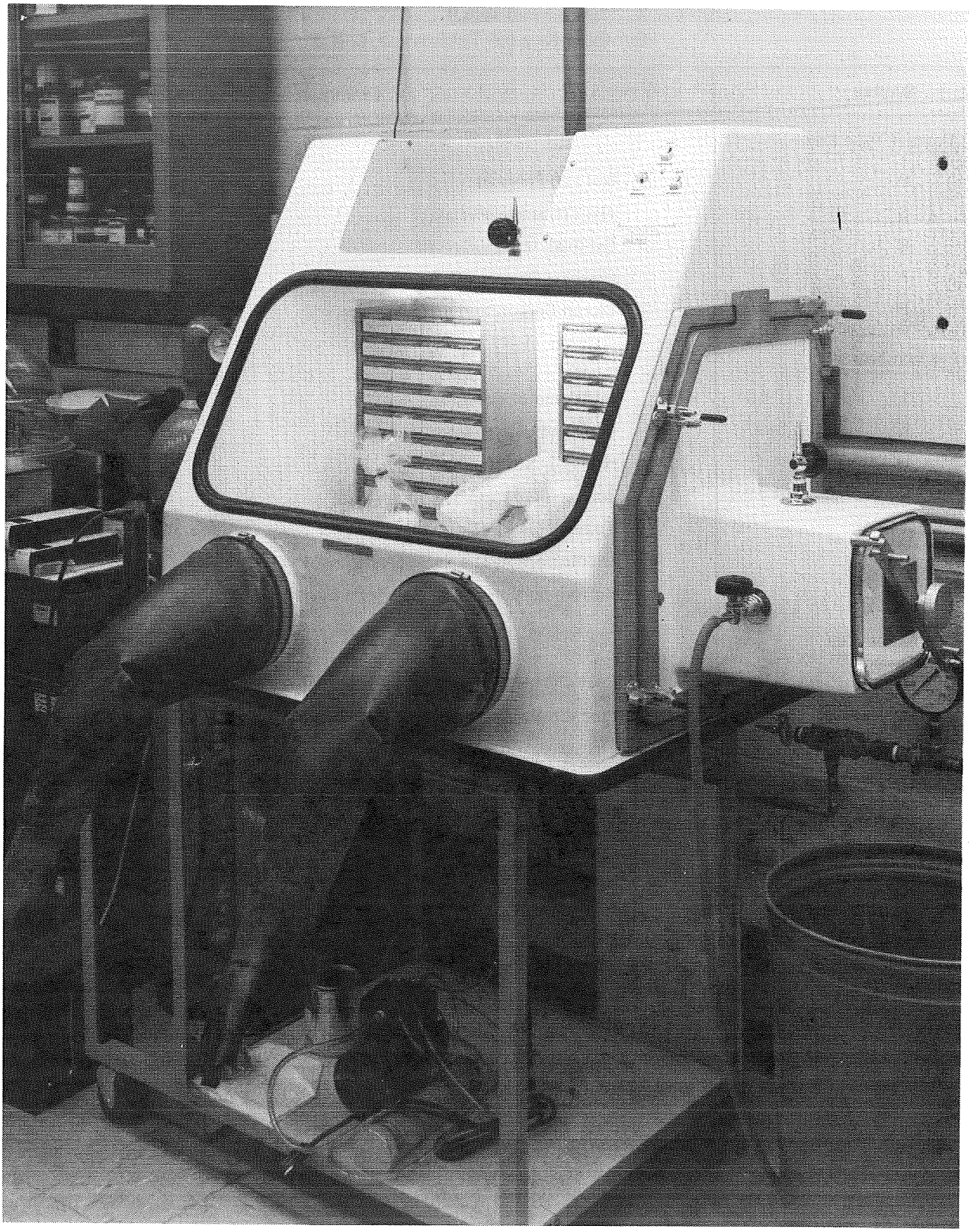

Figure 1. Receiving/storage station.

Thermal Conductivity

A model TPRC 100 thermal comparator made by McClure Park Corporation, West Lafayette, Indiana, was used for all thermal conductivity measurements.

The essential part of the thermal comparator is an insulated probe with a projecting tip. The probe is integral with a thermal reservoir held at a temperature about 15 to 20 K above room temperature. A surface thermocouple is mounted at the tip of the probe and is differentially connected to the thermal reservoir for measuring the temperature difference between the reservoir and the tip. In operation, the probe is gently placed on the surface of the test material. On contact of the probe tip of known thermal conductivity (k_1) and originally at temperature T_1 with the surface of the test material of unknown thermal conductivity (k_2) and at room temperature (T_2), the temperature of the probe tip drops quickly to an intermediate temperature (T), giving the expression:

$$\Delta T = (T_1 - T) = (T_1 - T_2)\left(\frac{k_2}{k_1 - k_2}\right)$$

This temperature difference is registered as the electromotive force (emf) reading of the differential thermocouple after a brief transient period (1 to 2 seconds) has elapsed.

From the emf readings of the test on a series of reference specimens of known thermal conductivity, a calibration curve is obtained, and the thermal conductivity of an unknown specimen can thus be determined graphically from the emf reading, using the calibration curve. Ebonite, Corning code 7740 glass, fused silica, A110AT titanium, 316 stainless steel, and Armco iron specimens supplied by the instrument manufacturer were used to calibrate the instrument. Precision of emf readings was 4 percent for the standards and 5.3 percent for all the NaI(Tl) measured. Because of the nonlinear relationship of thermal conductivity and the emf read from a calibration curve, a 5-percent emf precision resulted in a much larger (16 percent) uncertainty in measured thermal conductivity.

Thermal Shock

Thermal-shock resistance of single-crystal NaI(Tl) and Polyscin was determined by using oil- and air-quench tests to measure the critical temperature gradient at crack initiation (ΔT_c). The extent of consequent crack propagation was noted and used as an indication of crack propagation resistance. Results were compared with predictions made by using known or derived material constants for NaI(Tl) in an equation derived by Hasselman (reference 10) and elaborated on in references 11 through 16.

Oil Quenching

The nine-plate specimens described in Table 1 were about one-tenth the size of the crystal proposed for the EGRET scintillator. In addition, five 7.62- by 1.27-cm diameter rod specimens were tested. These specimens were duplicate ultimate shear rods. Four of these specimens were Polyscin, and

one was a single crystal. In addition, two 3.81- by 1.27-cm diameter Polyscin rods were tested. These specimens were made from broken ultimate shear specimens. Finally, nine 6.35-cm long by 2.54-cm square bars were made from broken MOR specimens and were tested. Five of these specimens were single crystals, and the remaining four were Polyscin.

Oil testing was done by using Penetone TPC cutting fluid as a medium. This fluid is a very low-viscosity oil in which NaI(Tl) is quite insoluable and is used by manufacturers as a coolant in machining this material. Haake type FS and FK constant temperature hot and cold circulating baths were used for heating and quenching. Capacity of each unit was about 1.5 liters of fluid. The volume of the largest specimen was 0.15 liters. Both baths had a <1 K thermal gradient across the 10 centimeters from one side of the bath to the other. Temperatures of the bath fluid were measured to within ±0.5 K.

Before testing, all specimens were closely inspected for flaws such as edge, face, or corner cracks. Flaw size and location were recorded for later use in fracture analysis.

The testing involved heating the specimens for 30 minutes to allow them to thermally equilibrate, then transferring them as rapidly as possible to the cold bath, increasing the temperature difference between the two baths, if necessary, by 2 K increments until fracture first occurred. The difference temperature between the two baths at fracture was assumed to be equal to the thermal gradient at the specimen surface.

Measured values of ΔT_c at fracture were compared with predicted values for the various geometries and critical flaw sizes using the relation (reference 10):

$$\Delta T_c = \left(\frac{\pi G (1 - 2\nu)^2}{2E \alpha^2 (1 - \nu^2)}\right)^{1/2} \left(1 + \frac{16 (1 - \nu^2) N\ell^3}{9(1 - 2\nu)}\right) \ell^{-1/2} \left(\frac{Bk}{ah_c}\right) \tag{1}$$

where

E = Young's modulus = 2×10^{10} N/m^2

ν = Poisson's ratio = 0.314

K_{IC} = critical stress intensity factor = 0.382×10^6 N/m$^{3/2}$

G = fracture energy = $K_{IC}^2/2E$ = 5.1 J/m^2

α = coefficient of linear thermal expansion = 47×10^{-6} K^{-1}

N = number of cracks per unit volume = 3×10^5 m^{-3}

ℓ = crack length (m)

B = a geometric factor (4.67 for rods, 4 for square bars, and 3.25 for square plates, reference 12)

k = thermal conductivity of NaI(Tl) = 1.71×10^{-2} W/cm K

a = characteristic length of specimen (volume to surface-area ratio) = 0.75, 0.54, and 0.29 cm for plate, bar, and rod specimens, respectively

h_c = calculated average surface heat-transfer coefficient, assuming forced convection in light oil = 0.019, 0.024, and 0.037 W/cm^2 K for plate, bar, and rod, respectively

As agreement between observed and calculated ΔT_c was good, the foregoing equation was used to calculate an average heat-transfer coefficient in still air, assuming a crack size equal to the average in Polyscin and an average ΔT_c observed for rod specimens tested in air.

Air Quenching

Two Polyscin rod and two Polyscin bar specimens were tested in air by heating the specimens in a convection oven for 30 minutes and then quenching into still room-temperature air (297 K). Temperature in the oven was read with a thermometer. The oven temperature was raised by 5 K increments until fracture occurred on quenching. The critical temperature (ΔT_c) was taken as the difference between oven temperature and room temperature. Thermal gradients in the oven were negligible over the dimensions of the specimen.

The effects of specimen size were evaluated by plotting ΔT_c versus surface area to volume ratio for both oil- and air-tested specimens.

Heat Capacity

The heat capacity of single-crystal and polycrystalline NaI(Tl) was measured at 310 K using a Perkin-Elmer differential scanning calorimeter model DSC-1B with a heat capacity kit (P–E part No. 219-0136). This instrument uses a comparative method to measure the amount of heat required to raise the temperature of a specimen to a specified temperature at a predetermined rate. In the determination, a sapphire standard, the specific heat of which is accurately known and documented, is used as a comparison material. The measurement is based on the electrical power required for maintaining the temperature control of a specimen and a reference pan embedded in a specimen-holder assembly block. The system monitors and controls the average temperature of the specimen-holder assembly block and the difference temperature between the reference holder and the specimen holder. Thus, by increasing the temperature of the specimen-holder assembly block to a specified value at a predetermined rate and monitoring the differential power needed for maintaining the same temperature in the specimen holder as in the reference holder, a measure of the energy supplied to the specimen and its holder is obtained relative to the reference holder and its contents, as a function of time or temperature.

In practice, the average temperature of the specimen-holder assembly block is recorded on the abscissa while the differential power needed for maintaining an equivalent temperature between the reference holder and the specimen holder is recorded on the ordinate of the system's chart recorder. This method involves (1) heating the specimen-holder assembly block to a predetermined temperature at a specified rate, using sapphire and an empty reference pan, (2) making a blank determination with both pans empty, and finally, (3) scanning the same range using the specimen and an

empty reference pan. In each determination, an ordinate pan shift from one baseline to a new baseline occurs. After correcting the ordinate amplitudes recorded for the specimen and the reference holder in light of the blank determination, the heat capacity of the specimen is calculated as:

$$C_p \text{ (specimen)} = \frac{A_s}{A_r} \times \frac{W_r}{W_s} \times C_p \text{ (sapphire)}$$

where

A_s = ordinate amplitude (specimen)

A_r = ordinate amplitude (sapphire)

W_r = weight (sapphire)

W_s = weight (specimen)

Precision (standard deviation divided by the mean) of the measurement was less than 2 percent. Table 1 describes the specimens.

Elastic Constants

Density was determined for NaI(Tl) compression specimens from first and second shipments by measuring their weight and dimensions inside the dry glove-box storage facility.

The elastic stiffness constants for single crystals, and Young's modulus and shear modulus for Polyscin specimens, were measured in two ways. The first and most accurate method used a Panametric model 5054 time intervalometer to measure the transmit time of an ultrasonic pulse in the material, using a technique called pulse-echo overlap. In this technique, an acoustic transducer is used to inject a shear or longitudinal wave packet into a specimen. The same transducer is then used to pick up the echo of the wave packet after it is reflected from a surface that is perpendicular to the transmission direction and that is situated at an accurately known distance from, and parallel to, the introduction plane. The transducer signal is applied to the vertical axis of an oscilloscope, and the horizontal axis of the oscilloscope is swept sinusoidally at a frequency whose period is the round-trip transit time of the wave packet, thus superposing the injected wave packet with its echo. Because the horizontal drive frequency can be generated and measured accurately, the time of flight of the wave packet can be determined accurately. The time between wave-packet injections was large and the period of vibrations within a wave packet was small compared with the round-trip time of a wave packet. This enabled multiple echoes to die out before new echoes were generated and enabled the injected wave packet and its reflections to be well-defined entities on the oscilloscope rather than interferring with one another. Longitudinal and shear wave transducers had a period of 0.44 μs. The time between wave-packet introductions was 0.01 or 0.001 times the typical round-trip flight times, which were 20 to 40 μs. Accuracy and precision of the measurement was 0.03 percent and was limited by the accuracy and precision of the measurement of specimen dimensions and density. Ultimate compression and MOR bend-test specimens were used for this measurement (Table 1).

The second method used to measure elastic moduli employed a Nametre model XV acoustic spectrometer to measure resonance frequencies of appropriately held specimens. In this technique, electromagnetic pickup and drive units (Airpax 1- 0055) are used to excite and monitor specimen vibrations. Small soft-iron contacts cemented to the specimen provide electromechanical coupling with the transducers. The specimens were supported on wire or point supports at nodal points using a chrome-plated brass frame designed for this use by Nametre. The frame itself was mounted on rubber and styrofoam padding to isolate it from spurious vibrations. The lathe-like specimens listed in Table 1 (measurement No. 5) were driven in flat-flexural and torsional resonance by appropriate placement of the driver and pickup transducers with respect to the specimen. Mechanical damping efficiency or internal friction (Q^{-1}) was also measured with the Nametre acoustic spectrometer, using the same lathe-like specimens. In the second shipment of material (Table 2), elastic moduli of only the eight Polyscin specimens were measured, and the method used the pulse-echo overlap technique.

The stiffness constants (C_{11}, C_{12}, and C_{44}) can be determined from the sound velocities of three independent waves in a single crystal using the pulse-echo overlap technique. The three types of waves that are most economical of specimens are those derived by measuring the longitudinal and two perpendicular shear velocities in the <011> direction on an ultimate compression specimen. For such specimens (reference 17, page 371),

$$C_{44} = V_{S1}^2 \rho$$

$$C_{11} = (V_L^2 + 2 V_{S2}^2 - V_{S1}^2) \rho$$

$$C_{12} = (V_L^2 - V_{S1}^2 - V_{S2}^2) \rho$$

where

V_{S1} = shear wave velocity in a face-diagonal direction such as <011> with displacement in a principal-axis direction such as <100>

V_{S2} = shear wave velocity in a face-diagonal direction such as <011> with displacement in a face-diagonal direction, such as $<0\bar{1}1>$

V_L = longitudinal wave velocity

ρ = density

The other approach to specimen utilization was to use both <100> and <111> ultimate compression specimens. In this case, the longitudinal and shear velocities were measured along the specimen axes. For these specimens, the shear wave velocity is rotationally invariant. In this case, for <100> specimens,

$$C_{11} = V_L^2 \rho$$

$$C_{44} = V_S^2 \rho$$

and for <111> specimens, using C_{11} and C_{44} calculated from the <100> specimen (reference 17, page 371),

$$C_{12} = (3\rho V_L^2 - C_{11} - 4C_{44})/2$$

and

$$C_{12} = C_{11} + C_{44} - 3\rho V_S^2$$

Both values of C_{12} were determined, and an average value was calculated. In both approaches to specimen utilization for measuring C_{11}, C_{12}, and C_{44}, values for the anisotropy constant (A) and the bulk modulus (B) were calculated as:

$$A = 2C_{44}/(C_{11} - C_{12})$$

$$B = 1/3\,(C_{11} + 2C_{12})$$

Values for Young's modulus in <100> principal-axis, <011> face-diagonal, and <111> body-diagonal directions were calculated using the following formula (reference 18, page 183):

$$E_{hkl}^{-1} = S_{11} + (2S_{12} - 2S_{11} + S_{44})(h^2k^2 + h^2l^2 + k^2l^2) \qquad (2)$$

where hkl are the direction cosines of the longitudinal displacement, or the axis of an axially stressed rod, and S_{ij} are the elastic compliances. The elastic compliances are related to the stiffness constants, C_{ij}, by:

$$S_{11} = (C_{11} + C_{12})/(C_{11} - C_{12})(C_{11} + 2C_{12})$$

$$S_{12} = -C_{12}/(C_{11} - C_{12})(C_{11} + 2C_{12})$$

$$S_{44} = 1/C_{44}$$

The shear modulus (G) and Poisson's ratio (ν) are dependent on crystallographic orientation in a manner similar to Young's modulus. The shear modulus is given by (reference 18, page 106):

$$G_{12}^{-1} = S_{44} + 4\,(2S_{12} - 2S_{11} + S_{44})(h_1k_1h_2k_2 + h_1l_1h_2l_2 + k_1l_1k_2l_2) \qquad (3)$$

where the subscript 1 on G^{-1} and on the direction cosines refers to the direction around which rotation occurs or along which a shear wave propagates, and subscript 2 refers to the direction of displacement (or more properly, for torsion, to the direction of the tangent to the displacement).

Similarly, Poisson's ratio is given by (reference 18, page 184):

$$\nu_{12} = - E_1 [S_{12} - 1/2 (2S_{12} - 2S_{11} + S_{44})(h_1^2h_2^2 + k_1^2k_2^2 + l_1^2l_2^2)]$$

where, in this case, the subscripts on ν, E and the direction cosines (hkl) again refer to directions. Subscript 1 refers to the direction of axial strain, subscript 2 refers to the direction of lateral strain, and ν_{12} is the ratio of lateral strain along direction 2 to axial strain along direction 1. In terms of the measured C_{ij}, the formulas for $E_{hk\ell}$, G_{12}, and ν_{12} are:

$$E_{hkl} = \left[E^{-1}_{<100>} + \frac{1}{C_{44}} (1 - A)\,\Omega\right]^{-1}$$

$$E^{-1}_{<100>} = \frac{(C_{11} + C_{12})}{(C_{11} + 2C_{12})(C_{11} - C_{12})}$$

$$\Omega = h^2k^2 + h^2l^2 + k^2l^2$$

$$G_{12} = \left[G^{-1}_{<100><010>} + \frac{4}{C_{44}} (1 - A)\,\Omega_{12}\right]^{-1}$$

$$G^{-1}_{<100><010>} = 1/C_{44}$$

$$\Omega_{12} = h_1k_1h_2k_2 + h_1l_1h_2l_2 + k_1l_1k_2l_2$$

$$\nu_{12} = E_1\left[\frac{C_{12}}{(C_{11} + 2C_{12})(C_{11} - C_{12})} + \frac{1}{2C_{44}} (1 - A)\,\Omega_{12}\right]$$

$$\Omega_{12} = h_1^2h_2^2 + k_1^2k_2^2 + l_1^2l_2^2$$

For polycrystalline specimens, the shear wave velocity is rotationally invariant, and only one longitudinal velocity (V_L) and one shear velocity (V_S) were measured. The formulas used to determine Young's modulus, the shear modulus, Poisson's ratio, and bulk modulus for these specimens were as follows (reference 19, page 18):

$$R = V_L/V_S$$

$$\nu = (R^2 - 2)/2 (R^2 - 1)$$

$$F = [(1 - \nu)/(1 + \nu)(1 - 2\nu)]^{1/2}$$

$$E = V_L^2 \rho / F$$

$$G = V_S^2 \rho$$

$$B = \rho \left(V_L^2 - \frac{4}{3} V_S^2 \right)$$

The other technique for measuring elastic constants and moduli was to determine resonant frequencies of vibration of appropriately held specimens, using an acoustic spectrometer. The elastic modulus calculations using measured resonant frequencies, specimen dimensions, and density are an iterative process and were done on a computer.

For a rectangular bar of material, Young's modulus (E) and shear modulus (G) are calculated from the flat-flexural fundamental and torsional fundamental as (reference 18, pages 84 and 90):

$$E = 0.94642 \left(\frac{\ell^2 f_E}{h} \right)^2 \rho T_3$$

$$G = 4 \rho R \ell^2 f_G^2 / n$$

where

E = Young's modulus (dynes/cm^2)

G = shear modulus (dynes/cm^2)

ρ = density (g/cc)

n = order of vibration = 1

f_E = flat-flexural fundamental (Hz)

F_G = torsional fundamental (Hz)

ν = Poisson's ratio

ℓ = specimen length (cm)

h = specimen height (cm)

b = specimen breadth (cm)

T_3 and R are finite length correction factors.

$$T_3 = 1 + 6.585\,(1 + 0.0752\,\nu + 0.8109\,\nu^2)\left(\frac{h}{\ell}\right)^2 - 0.868\left(\frac{h}{\ell}\right)^4 - \frac{8.340\,(1 + 0.2023\,\nu + 2.173\,\nu^2)\left(\frac{h}{\ell}\right)^4}{1 + 6.338\,(1 + 0.14081\,\nu + 1.536\,\nu^2)\left(\frac{h}{\ell}\right)^2}$$

$$R = \left(\frac{1 + (b/h)^2}{4 - 2.521\,(h/b)\left(1 - \left(\frac{1.991}{e^{\pi b/h} + 1}\right)\right)}\right)\left(\frac{1 + 0.00851\,n^2b^2}{\ell^2}\right) - 0.060\left(\frac{hb}{\ell}\right)^{3/2}\left(\frac{b}{h} - 1\right)^2$$

From these values of E and G, Poisson's ratio is calculated as (reference 19, page 89):

$$\nu = \frac{E}{2G} - 1$$

Since ν appears in the calculation for E, the procedure for calculating Young's modulus is to assume an arbitrary value of ν equal to 0.3 in the calculation for E, then determine G and calculate ν from the above equation, and iteratively arrive at a value for E. This iterative process is done by computer to less than 0.1-percent change in ν. The accuracy and precision of the measurement was limited by how closely the resonant frequency could be read and by positioning the specimen grips. It is estimated that an accuracy and precision of about 1 percent was obtained.

For single-crystal specimens, E and G are calculated as for Polyscin above. The elastic compliances are then calculated from the directional Young's modulus and shear modulus given by equations 2 and 3. For <100> specimens,

$$E^{-1}_{<100>} = S_{11} \text{ and } G^{-1}_{<100><010>} = S_{44}$$

This gives two of the three elastic compliances. Compliance S_{12} is calculated by using the values of E iteratively derived for the <011> and <111> specimens and using the above-determined values for S_{11} and S_{44} from a <100> specimen. For a <011> specimen,

$$S_{12} = 2\,(E^{-1}_{<011>} - \frac{1}{2}\,S_{11} - \frac{1}{4}\,S_{44})$$

Similarly, for a <111> specimen,

$$S_{12} = \frac{3}{2}\left(E^{-1}_{<111>} - \frac{1}{3} S_{11} - \frac{1}{3} S_{44}\right)$$

With S_{11}, S_{12}, and S_{44} so determined, values of C_{11}, C_{12}, and C_{44} are now available as (reference 23, page 147):

$$C_{11} = (S_{11} + S_{12})/(S_{11} - S_{12})(S_{11} + 2S_{12})$$

$$C_{12} = -S_{12}/(S_{11} - S_{12})(S_{11} + 2S_{12})$$

$$C_{44} = 1/S_{44}$$

This method is more complex and not as accurate as the pulse-echo overlap method that can be used to determine the stiffness constants (C_{ij}) directly from velocity data without first computing the elastic compliances (S_{ij}).

Internal friction (Q^{-1}) was determined at flexural, torsional, and longitudinal fundamentals and their overtones by two independent methods, using the Nametre model XV acoustic spectrometer as described in reference 20. One method used forced vibration at resonance, relating internal friction to the half-peak width of the resonance curve of frequency versus amplitude. The second method used the log-decrement of amplitude as a measure of the damping of free vibrations in the specimen at resonance. These methods generated internal friction data in the 700- to 50,000-Hz range. The same setup used to measure elastic properties was used to measure damping.

The forced-vibration measurement of Q^{-1} involves obtaining a spectrum of vibrational amplitude (indicated by the output voltage of the pickup detector) as a function of frequency while the specimen is driven through a range of frequencies around resonance. Internal friction (Q^{-1}) is calculated from the width of the resonance peak at half its maximum height, as follows (reference 20, page 121):

$$Q^{-1}_{\text{forced}} = \frac{\Delta f}{f_r\sqrt{3}}$$

where

f_r = resonance frequency (Hz)

Δf = width of the resonance peak at half-height (Hz)

To measure Q^{-1} by the free-vibration method involves measuring the decay of free vibrations at resonance after the driving force is removed. The drop in amplitude as a function of time is used to calculate Q^{-1} as follows (reference 18, page 121):

$$Q^{-1}_{\text{free}} = \frac{\ln A_2/A_1}{\pi f_r \Delta t}$$

where

A_2/A_1 = ratio of amplitudes of any two successive vibrations

Δt = time elapsed between A_1 and A_2 (sec)

The results of forced-vibration measurements of Q^{-1} were used to assess material effects on Q^{-1} because these measurements reflect Q^{-1} measured at the maximum amplitude attained by the specimen. Free- and forced-vibration measurements were averaged to assess the frequency dependence of Q^{-1}, using free-vibration estimates of Q^{-1} at maximum amplitude. Finally, in describing observed amplitude dependence of Q^{-1}, only the free-vibration results were used because they yield a decay curve from which Q^{-1} can be correlated easily with relative vibrational amplitude.

Ultimate Strength

Modulus of rupture, ultimate shear, and compression strength measurements and K_{IC} of NaI(Tl) were all done with a floor-model 1125 Instron universal tester that had been modified to provide a low-humidity environment. The modification enclosed the loading frame with sealed acrylic sheets that had two gloved ports for manipulating specimens and a flapped iris port for specimen entry. Dry N_2 from a liquid nitrogen dewar was used to purge the test region. In addition, a dryer train continuously recirculated the chamber atmosphere through anhydrous $CaSO_4$. The method provided a less than 3-percent RH environment at room temperature. Stress-rate testing and the critical stress-intensity factor (K_{IC}) of Polyscin NaI(Tl) was measured at NBS using a similarly enclosed Instron testing machine. The NBS system, however, did not require the $CaSO_4$ recirculation system because of its smaller size.

The equipment used for the GSFC MOR tests is a modification of the four-point bending fixture shown in Figure 2. Extensions were built onto the lower bearing rollers of the fixture, and a dummy specimen was mounted on these extensions during each test to account for fixture compliance. The motion of the fixture was electronically subtracted from the motion of the specimen by subtracting the dummy specimen linear variable-differential transformer (LVDT) output from the NaI(Tl) specimen LVDT output. The fixture had a 10.15-cm outer span and a 3.39-cm inner span. Specimens were broken using a crosshead speed of 0.00508 cm/minute. The specimens tested are described in Tables 1 and 2. Nominally, the specimens were 12.7- by 2.54- by 2.54 cm prisms. For these specimens, the calculated applied stress rate is 0.1956 MPa/s. For single-crystal material, specimens were oriented with their long axis along one of the three crystallographic symmetry axis directions, <100>, <011>, or <111> and were pushed in the <001>, $<0\bar{1}1>$, and $<1\bar{1}0>$ directions, respectively, as shown in Figure 3. The observed failure tensile stress was resolved into a component normal to the observed failure plane. The properties measured from the loading curves and LVDT data were modulus of rupture, proportional limit, and maximum deflection before failure. After failure pieces of the specimen were dissolved in nitric acid and thallium concentration, measurements were made using a Perkin-Elmer model 403 atomic-absorption spectrometer.

The purpose of NBS MOR stress-rate testing was to assess the susceptibility of NaI(Tl) to subcritical crack growth. If subcritical crack growth occurs, specimens broken at a high stress rate appear to be stronger than specimens broken at a low stress rate due to crack extension during the loading process. The NBS modulus-of-rupture equipment was similar to that of the GSFC facility except that

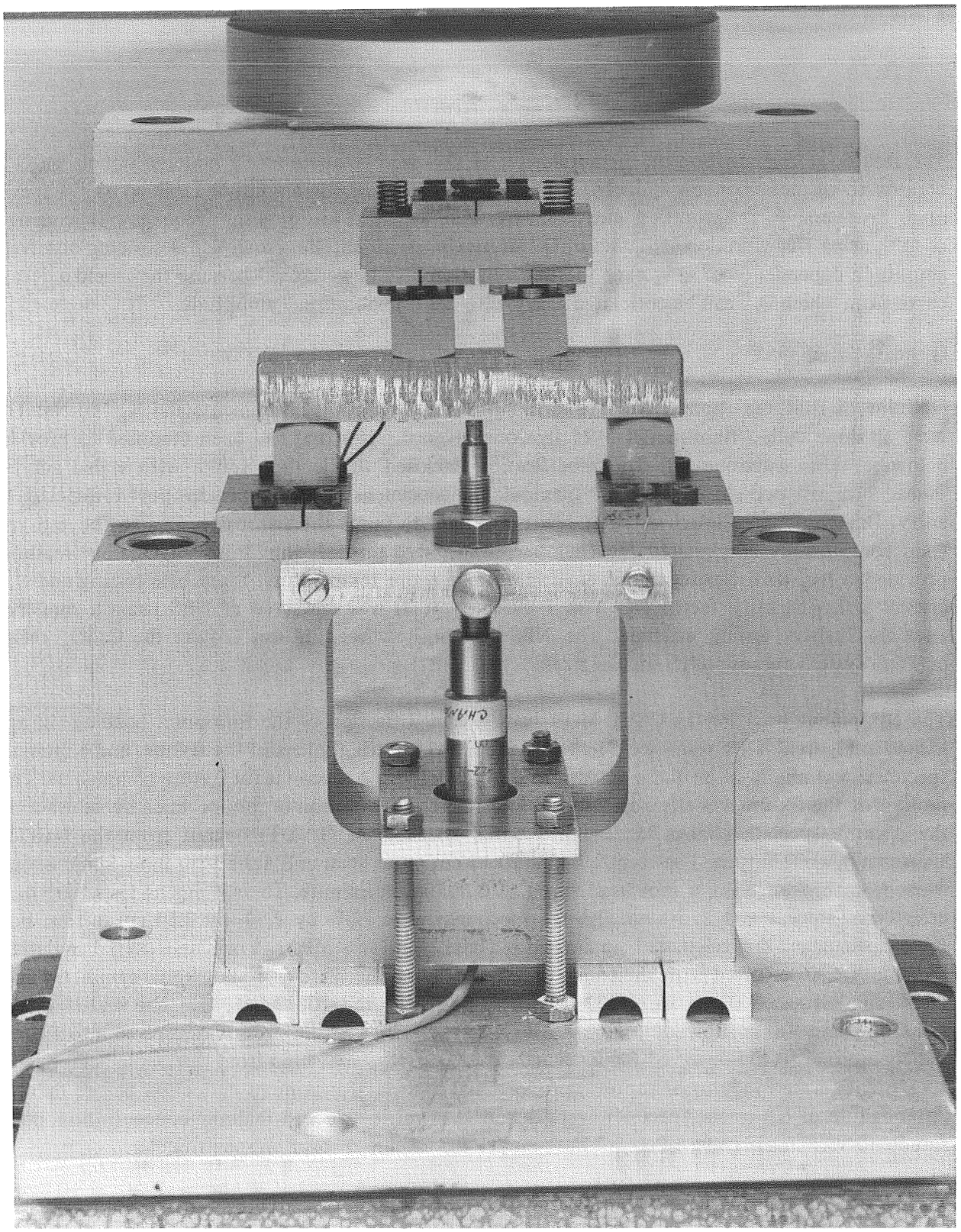

Figure 2. Closeup of the MOR test fixture used in test 6a (Table 1).

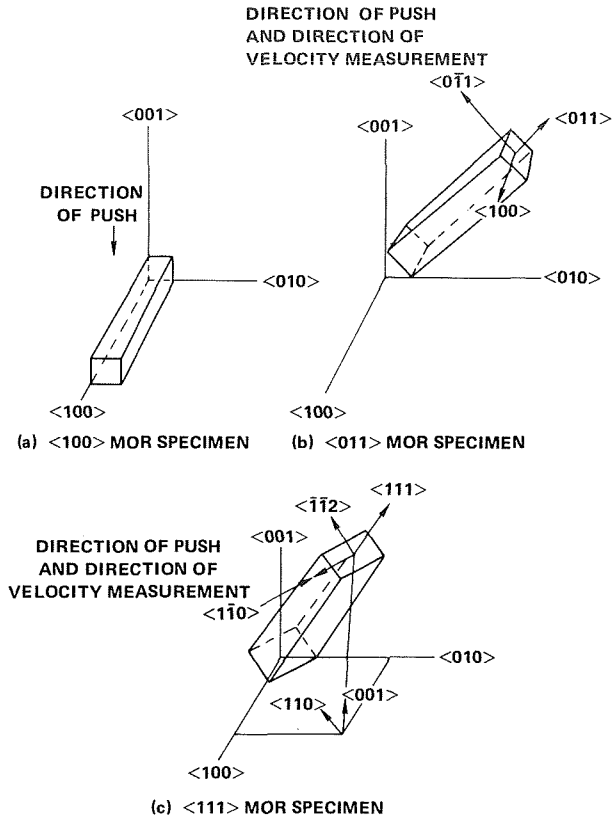

Figure 3. Diagram of single-crystal MOR specimen orientations.

the test fixture had three-point loading with a span of 2.15 cm. In addition, the specimens were smaller (Table 3), being nominally 2.5 by 0.6 by 0.3 cm. Crosshead rates of 5.08×10^{-1}, 5.08×10^{-2}, 5.08×10^{-3}, and 10.16×10^{-4} cm/minute were used. In addition to the modulus of rupture, the 0.2-percent offset proportional limit was determined for loading rates of 5.08×10^{-1}, 5.08×10^{-3}, and 10.16×10^{-4} cm/minute.

Shear-strength tests were made by using a double-shear fixture that is shown schematically in Figure 4a. The fixture could also be used in single shear as shown in Figure 4b. Machine crosshead speeds of 0.0127 cm/min and 0.0508 cm/min were used. The specimens were nominally 1.27-cm diameter, 7.62-cm long rods, as indicated in Table 1.

Compression testing of NaI(Tl) at GSFC was performed in the enclosed Instron facility with a self-aligning loading fixture shown schematically in Figure 5. To prevent localized crushing from occurring at the ends, each specimen was placed into 0.158-cm thick end plate. At the beginning of each test, a crosshead speed of 0.00508 cm/minute was used until the 0.2-percent yield point had been reached. As the test continued, the crosshead speed was incrementally increased from 0.00508 to 0.127 cm/minute until cracking began and, finally, load-bearing capability was lost. Initial cracking was observed visually, using a high-intensity lamp. The increase in strain rate was necessary because most specimens exhibited a total strain greater than 20 percent. From load-deflection curves recorded

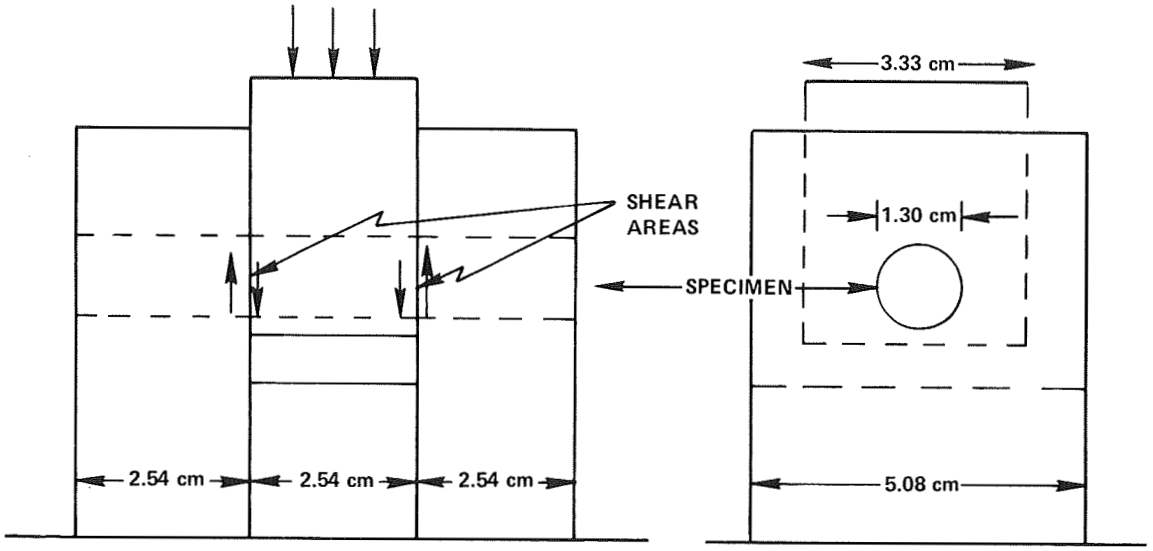

(a) DOUBLE-SHEAR FIXTURE

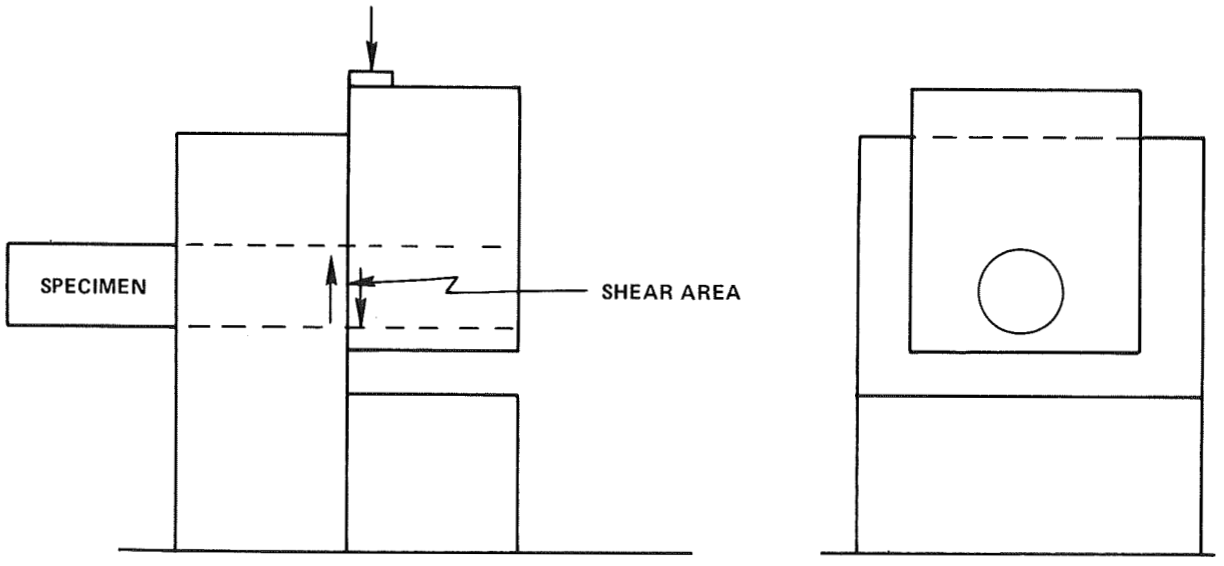

(b) SINGLE-SHEAR FIXTURE

Figure 4. Full-scale drawing of test fixtures.

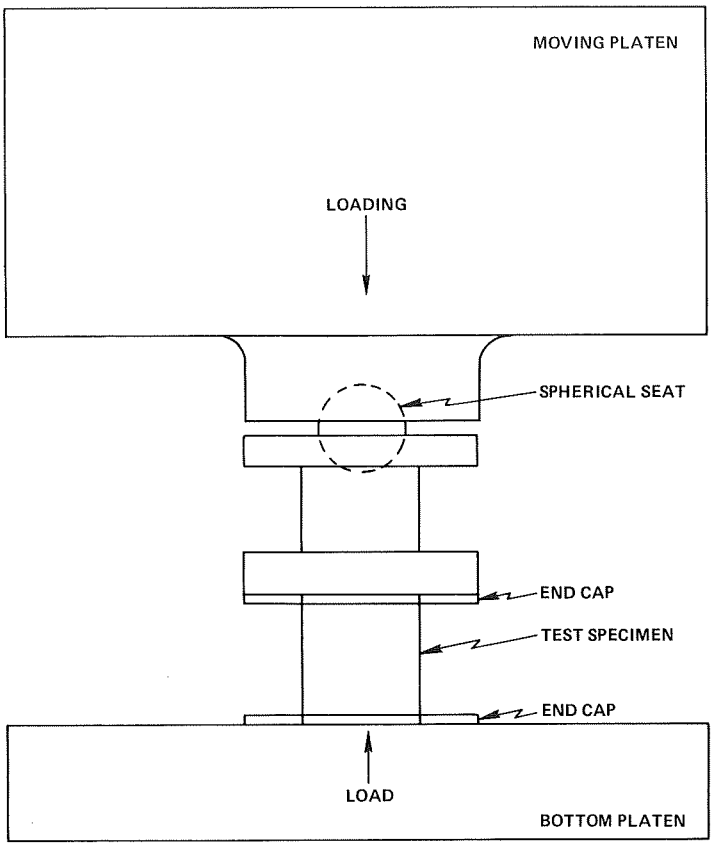

Figure 5. Schematic of loading fixtures used in compression testing of sodium iodide.

by the testing machine, proportional elastic limit stress, 0.2-percent compressive yield stress, ultimate compressive stress, initial cracking stress, and total compressive strain were determined for first-shipment material (Table 1), but only initial cracking stress was determined for second-shipment material (Table 2).

Compressive testing of CsI(Na) at NBS was performed with equipment similar to that used at GSFC except that again the specimens were smaller, nominally 1.27 cm long by 0.635 cm in diameter (Table 3). These specimens were not stressed to the point of load-bearing loss as were the NaI(Tl) specimens. The 0.2-percent offset yield stress was the only property measured because these specimens were subsequently used for creep measurements. Although no purged dry N_2 enclosures were used for CsI(Na) testing, the specimens were dip-coated in silicone oil (Dow Corning type 704) to provide a vapor barrier. Tests were performed using a table-model Instron TM-M-L. A crosshead travel rate of 0.5 cm/minute was used. A specimen fixture, based on a V-block, was developed to locate the test specimen on and parallel to the axis of the test frame. After the yield measurement, the specimens were examined for evidence of distortion.

The critical stress-intensity factor (K_{IC}) of Polyscin NaI(Tl) was measured in two ways: (1) using the double-cantilever-beam technique, and (2) using the notched-beam technique. The measurement was initially made at NBS using the double-cantilever-beam method that is described in reference 21,

page 24. A schematic diagram of the specimen and the formula used to calculate K_{IC} are shown in Figure 6. Specimens were nominally 0.2- by 1.9- by 5.0-cm plates (Table 3). The load was applied through wire hooks epoxied to the end of the plate. The specimens were placed in the Instron test chamber at a dew point of 240 K. A beginning crack was introduced into the specimen by tapping a razor blade into one end. The specimens were stressed in the test machine at a crosshead speed of 0.0508 cm/minute until the crack propagated. Although all the cracks propagated out to the side rather than down the center of the specimens, a value of K_{IC} was calculated for the initial stages of growth from the peak load, specimen dimensions, and crack length using the formula shown in Figure 6.

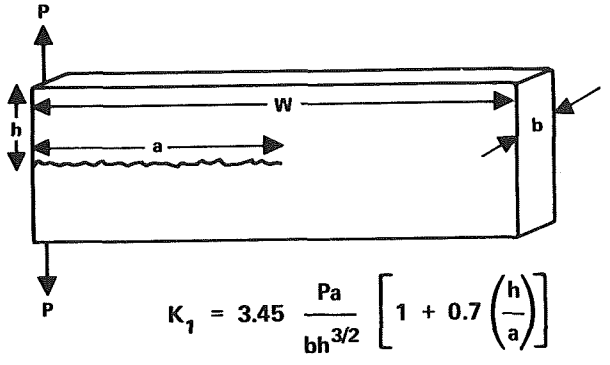

Figure 6. Double-cantilever-beam specimens (reference 21)

The second method for measuring K_{IC} was a single-edge notched-beam test performed at GSFC using broken MOR specimens. The technique is discussed in reference 22, page 13, and a schematic diagram of a specimen with the formula used to calculate K_{IC} is shown in Figure 7. The test is a three-point bend test with a notch at the center of the tensile face. Specimens of various sizes, but geometrically similar, were tested. Geometric similarity was maintained by keeping the ratio of span-to-specimen thickness and notch-depth-to-specimen thickness constant at 4 and 0.30, respectively.

To preclude geometric effects and ensure accurate measurement of K_{IC}, a ln ln plot of failure stress versus notch depth was made, and the slope was compared to -1/2. Specimens were notched with a 0.043 cm thick wafering wheel and were tested in a variable-span three-point bend fixture at a crosshead speed of 0.127 cm/minute. Tests were conducted in less than 3-percent RH at room temperature.

Creep

The creep apparatus and enclosure for NaI(Tl) testing was custom-built. It was determined that nine flexure tests and nine compression tests were required over a 6-month period. A schematic diagram of the test facility is shown in Figure 8. The facility was continuously purged with dry N_2. However, because of its size and the permeability of the acrylic enclosure to moisture, a gas-recirculating system was built. Humidity and temperature control was achieved at less than 1-percent

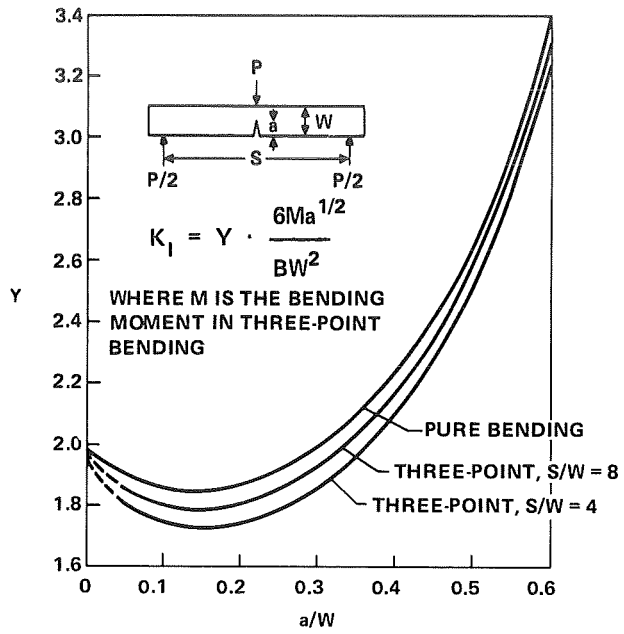

$$Y = K_I BW^2/6Ma^{1/2}$$

$$= A_0 + A_1 (a/W) + A_2 (a/W)^2 + A_3 (a/W)^3 + A_4 (a/W)^4$$

The coefficients A have the following values:

	A_0	A_1	A_2	A_3	A_4
Pure bending	+1.99	-2.47	+12.97	-23.17	+24.80
Three-point:					
S/W = 8	+1.96	-2.75	+13.66	-23.98	+25.22
S/W = 4	+1.93	-3.07	+14.53	-25.11	+25.80

Figure 7. K calibrations for bend specimens (reference 22).

RH and 300 K with two removable dryer/heater units, one of which is depicted in Figure 9. Each unit contained 4 pounds of anhydrous calcium sulfate. Two fans within each dryer recirculate the atmosphere within the RTV-sealed acrylic enclosure that covers the creep facility. Also within the recirculating unit is a thermostatically controlled cone heater for maintaining the temperature within the enclosure at 300 K. Sliding doors seal off the dryers from the enclosure for servicing and for regenerating the dryer material every 72 hours. Two units, one at each end of the enclosure, are capable of dropping the humidity of the N_2 gas in the enclosure from 25- to 0.5-percent RH in 2 hours.

Inside the creep facility, fixtures were suspended from an I-beam frame mounted on a 1.22- by 1.83-m pneumatically suspended isolation table. The fixtures were dead-weight loaded. To accommodate 18 simultaneous tests, six multiple-specimen fixtures were made, each designed to allow testing three specimens with one set of weights, as shown in Figure 10. In each case, the load is applied at the bottom of the fixture and is transferred through the lower specimen to the middle specimen,

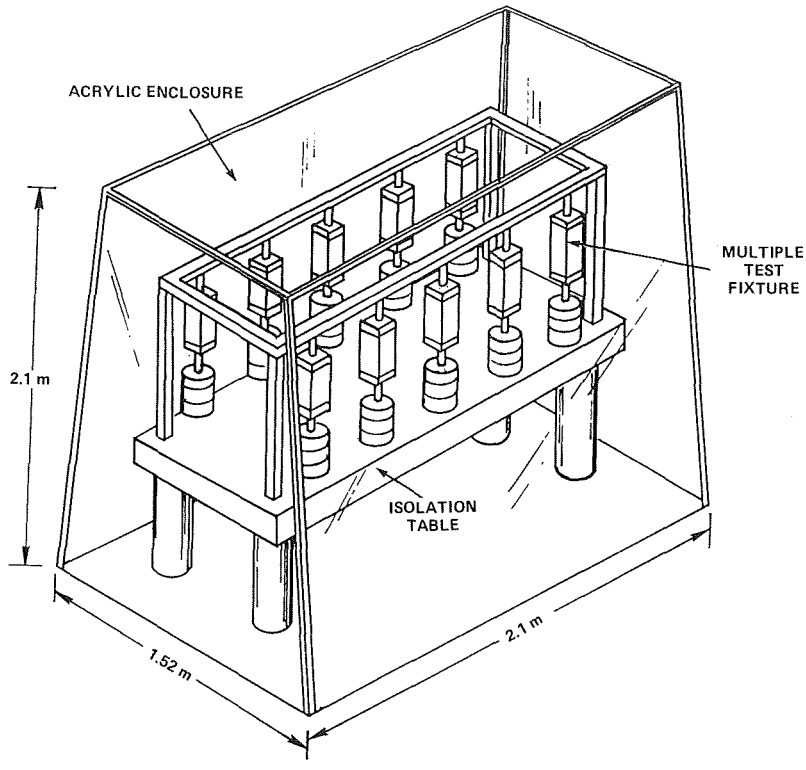

Figure 8. Multiple-creep-test facility.

through to the upper specimen, and finally to the upper fixture in a chain-like fashion. Creep displacements were measured with a Pickering model 7303W-4A0, 6-volt input dc-dc linear variable-differential transformer, which gives a 0- to 2-volt dc output for a 0- to 0.508-mm displacement with a sensitivity of 0.508×10^{-3} mm.

Initially, the middle fixture in each assembly was loaded to twice the nominally expected maximum service stress for the EGRET scintillator. The maximum expected service stresses were 1.29 MPa in flexure and 0.710 MPa in compression. In compression, stresses applied by the top and bottom fixtures in a loading chain were about 20 percent more and less, respectively, than the stresses applied by the middle fixture in an assembly. In bending, loading of the top and bottom fixtures in a chain differed from the middle fixture by about 30 percent.

The loading schedule for the assembly is shown in Table 5. As time progressed and some of the specimens were not observed to creep, the applied load was increased. Creep behavior was analyzed in terms of $(\text{time})^{1/3}$ equations:

$$\epsilon = a + bt^{1/3} \qquad \text{compression}$$

$$\delta = a + bt^{1/3} \qquad \text{flexure}$$

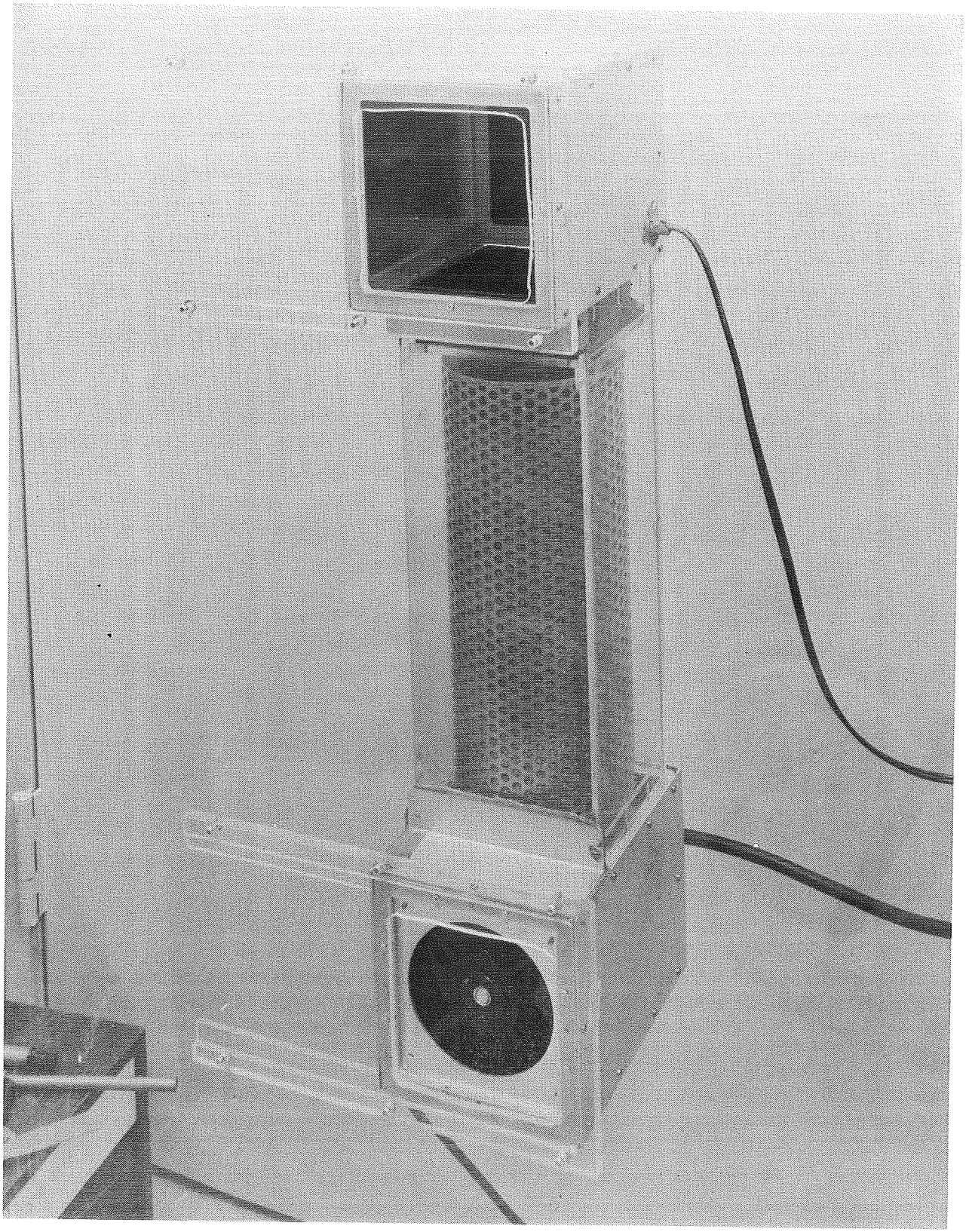

Figure 9. Dryer/heater unit for enclosures.

Figure 10. A portion of the multiple-creep test showing 12 flexure fixtures.

Table 5
Creep Loading Schedule

Type Test	Specimen Number	Specimen Designation	A: Applied Stress (MPa)	B: Initial Cracking Stress (MPa)	% of Initial Cracking Stress (A/B) X 100	C: Proportional Limit (MPa)	% of Proportional Limit (A/C) X 100
Compression	1	FS//	1.65	18.88	8.7	3.44	48
	2	FS//	1.38		7.3		40
	3	FS//	1.10		5.8		32
	4	IH⊥	1.65	12.46	13	2.43	68
	5	IH⊥	1.38		11		56
	6	IH⊥	1.10		8.8		45
	7	<111>	1.65	50.02	3.3	4.37	38
	8	<011>	1.38	38.52	3.5	4.94	28
	9	<100>	1.10	13.45	8.1	1.63	67
Flexure	10	FS//	3.36	3.92	86	2.89	116
	11	FS//	2.60		66		90
	12	FS//	1.85		47		64
	13	IH⊥	3.36	4.79	70	3.35	100
	14	IH⊥	2.60		54		78
	15	IH⊥	1.85		39		55
	16	<111>	3.36	6.79	49	2.21	152
	17	<011>	2.60	3.70	70	1.93	135
	18	<100>	1.85	2.50	74	1.91	96

where

t = time

ϵ = strain

δ = midspan deflection

b = slope of a $t^{1/3}$ plot

a = intercept of a $t^{1/3}$ plot

Flexure fixtures used four-point bending with an inner and outer span of 3.38 and 10.16 cm, respectively. Specimens were nominally 12.7 cm long with a 1.9-cm-square cross section (Table 1).

Compressive creep of CsI(Na) was measured by the NBS. However, a purged dry N_2 enclosure was not required as it was with NaI(Tl). Specimens were coated in silicone oil as for MOR measurements. The apparatus for this measurement was also custom-built and is shown in Figure 11. Four

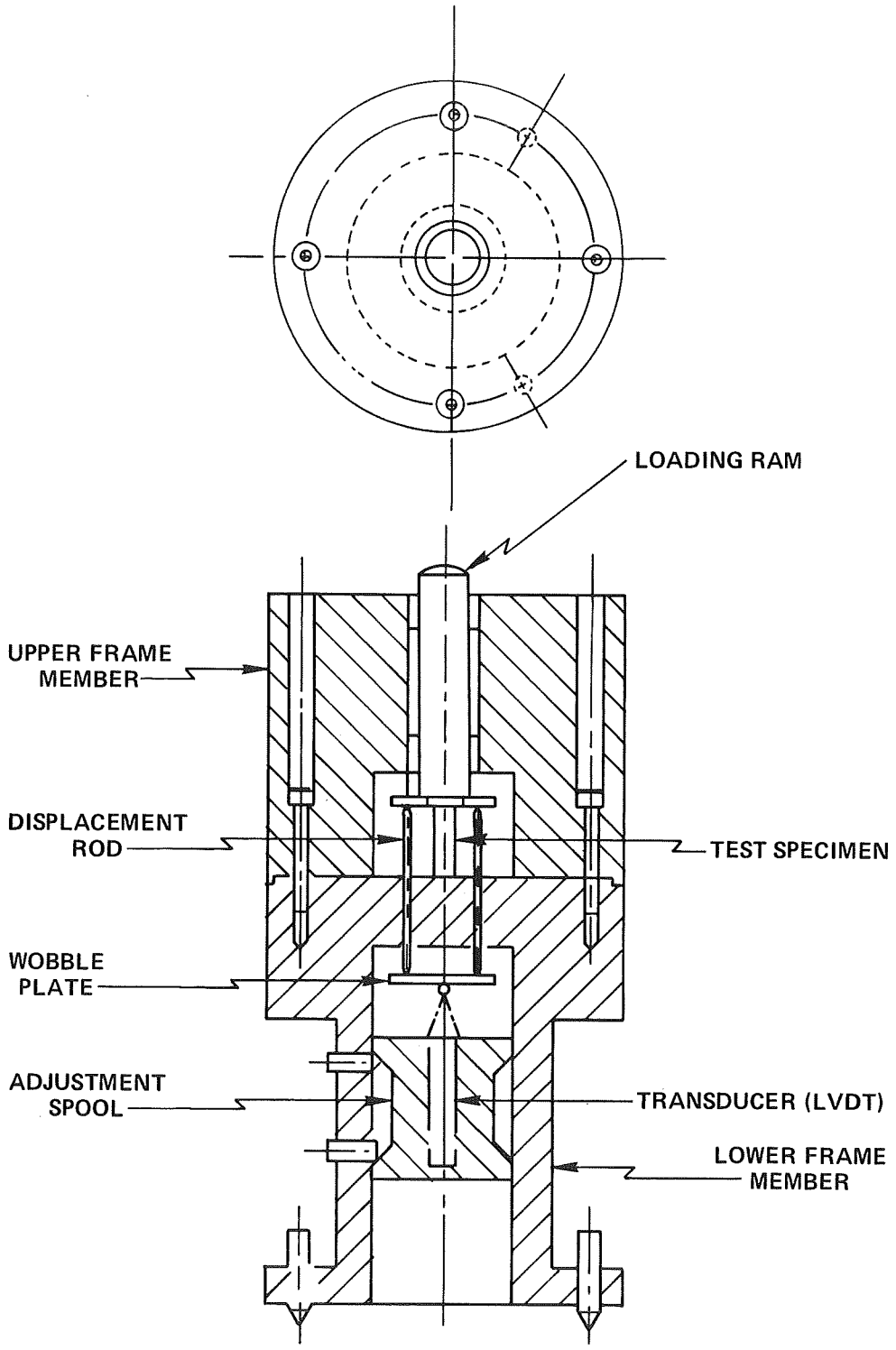

Figure 11. A one-half scale cross-sectional view of the CsI(Na) creep test frame.

test frames were built. The displacement transducers were LVDT-type transducers (Schaevitz Engineering model PCA-220-100), which have a displacement resolution of 0.003 mm and a less than 0.1 percent deviation from linearity. The use of a wobble-plate linkage to couple the specimen and the transducer provides a means of averaging out errors in the signal that result from misalignment of the specimen.

The CsI(Na) creep data were collected manually and were plotted using Dataplot (reference 9). Dataplot is an NBS-developed statistics, curve-fitting, and graphics program. The data were plotted in terms of a natural logarithm of time equation:

$$\epsilon = a_1 + a_2 \ln (1 + t/a_3)$$

where a_1, a_2, and a_3 are curve-fitting parameters.

To perform extrapolations of the test results, another computer program, Runnonlin, was developed (reference 9). Using Runnonlin, the test results were extrapolated to times outside the test data base with confidence limits based on the test-data scatter.

Hardness

Vickers microhardness of NaI(Tl) was measured using loads of 100, 300, and 500 g. The specimens were cleaned with toluene before indenting to remove any surface hydration, and no attempt was made to control relative humidity below laboratory ambient. The specimens were oriented so that their surface was perpendicular to the indenter and were aligned so that dimensions of the square-shaped surface impression were parallel to known crystallographic directions. Vickers hardness (H_v) was calculated using the equation:

$$H_v = 18.54\, P/d^2 \ [kg/mm^2]$$

where

P = load in grams

d = mean diagonal of indentation in μm

Susceptibility to Subcritical Crack Growth

In addition to the stress-rate testing of Polyscin performed by NBS and described under modulus-of-rupture ultimate strength testing, GSFC performed three-point instrumented impact tests on single crystals of NaI(Tl). An analog oscilloscope trace of the impact event was recorded as a load-time trace and was evaluated to obtain load to failure and time to failure. From these measurements, failure stresses and stress rates were calculated. Most specimens were cleaved from broken MOR bars. In addition, four 76- by 13- by 13-mm specimens were provided gratis from Bicron Corporation specifically for this test. Impact specimens of various dimensions were cleaved from these single-crystal bars by hand using a razor blade. After cleaving, the specimens were wet-ground and polished

by hand using a fixture to maintain parallel sides. Pentone Corporation's TPC solvent and General Electric's silicone (SF97-50) oil were used for grinding and polishing mediums, respectively. Specimen edges were chamfered. The long axis of a specimen was in the <100> direction, and prismatic surfaces were perpendicular to the other two principal axes. The majority of specimens were nominally 6.4 by 6.4 by 64 mm. A total of 22 of these specimens were tested.

The impact tester was a modified Custom Scientific Instruments, Incorporated, pendulum-type tester. The machine was modified by changing the impact mode from tension to three-point bending with a 50.8-mm span. A piezoelectric quartz load cell (Kister model 910) was used to pick up the impact event. The oscilloscope was externally triggered by the interruption of a helium/neon laser beam to a solar cell by a metal flag attached to the pendulum head. The impact tester was enclosed in a sealed acrylic chamber that had four flapped-iris ports for access. Surgical gloves were worn when handling the specimens. Specimens were broken at stress rates ranging from 1.0×10^4 to 4.0×10^4 MPa/s, compared with quasi-static stress rates of about 0.1956 MPa/s measured with a universal testing machine.

Ingot Variation

For NaI(Tl), ingot variation was investigated in a controlled manner (i.e., the same specimen sizes, test equipment, personnel, etc.) in terms of elastic moduli, modulus of rupture (MOR), and compressive initial cracking strength. This was done by measuring these properties for two Polyscin extrusions and by measuring the MOR of material from eight single-crystal ingots and the elastic constants for material from two of these single-crystal ingots. An uncontrolled measure of ingot variation of strength was obtained by comparing MOR values measured at GSFC with MOR values measured at NBS in stress rate testing to assess susceptibility to subcritical crack growth and with some early Polyscin strength measurements performed by Stanford University.

For CsI(Na), ingot variation was investigated by comparing compressive strength (0.2-percent yield) and creep for three single-crystal ingots and for polycrystalline material from a fourth ingot.

TEST RESULTS AND STATISTICAL ANALYSIS

Specimens were classified and differentiated on the basis of:

- Material type—NaI, CsI, polycrystal, or single crystal
- Ingot—Four Polyscin ingots, eight single-crystal ingots
- Position within an ingot—Initial and final end, surface, or interior of a Polyscin extrusion or top, middle, and bottom of a CsI ingot as designated in Table 4
- Orientation—Specimen dimensions relative to symmetry axes as designated in Table 4

In most cases, a statistical analysis determined whether observed differences in the mean value of a property for various classifications of material were significant. This analysis was done by pair-wise t-testing for significance of differences in mean values, after an F-test for equality of variances was

performed to ensure the validity of the t-test (reference 24, pages 61-65). In cases in which variances are not equal, another statistic (t′) is used rather than the t-variable for testing the hypothesis of equality of means (reference 25, page 264). In the following, the letter s refers to the square root of a sample variance, commonly called the standard deviation.

The F-test is as follows:

$$\text{hypothesis } H_o\text{: } S_{P1}^2 = S_{P2}^2 \text{ versus } H_1\text{: } S_{P1}^2 \neq S_{P2}^2$$

where S_{P1}^2 and S_{P2}^2 are population variances.

Accept H_o if:

$$\frac{S_1^{\,2}}{S_2^{\,2}} < F_c\,(\gamma, n_1 - 1, n_2 - 1)$$

where $S_1^{\,2}$ and $S_2^{\,2}$ are sample variances with $S_1^{\,2}/S_2^{\,2} > 1$, n equals the number of data points in each sample, and γ is the confidence level.

If the test statistic $(S_1^{\,2}/S_2^{\,2})$ is less than F_c, then H_o is accepted, and the mean value for each set of observations is compared using the t-test of equality of means. In this test, the hypotheses are:

$$H_o\text{: } \bar{X}_1 = \bar{X}_2 \text{ versus } H_1\text{: } \bar{X}_1 \neq \bar{X}_2$$

where $\bar{X}_1$ and $\bar{X}_2$ are means of samples X_1 and X_2.

H_o can be rejected if

$$t_c\,(\nu, \gamma) < \frac{\bar{X}_1 - \bar{X}_2}{S_p\sqrt{\frac{1}{n_1} + \frac{1}{n_2}}} = t_o$$

where

t_o = the test statistic

ν = number of degrees of freedom = $n_1 + n_2 - 2$

$S_P^{\,2}$ = pooled sample of variance = $\left[(n_1 - 1)\,S_1^2 + (n_2 - 1)\,S_2^2\right]/(n_1 + n_2 - 2)$

If the test statistic S_1^2/S_2^2 is greater than F_c, then the mean value for each set of observations is compared using test statistic t' rather than t_o in the t-test of equality of means, where:

$$t' = \frac{\bar{X}_1 - \bar{X}_2}{\sqrt{\bar{S}_1^2 + \bar{S}_2^2}} \quad \text{with } \bar{S}_1^2 = S_1^2/n_1, \bar{S}_2^2 = S_2^2/n_2$$

Coefficient of Linear Thermal Expansion (NaI(Tl) 253 to 323 K)

Measurements were made on three oriented single-crystal and four Polyscin NaI(Tl) specimens. Two determinations α_1 and α_2 were made for each specimen and the results are shown in Table 6.

Table 6
$\alpha \times 10^6$ (K^{-1})

Orientation* / Comment	Group 1		Group 2		Group 3		
	IH //	FH //	IS ⊥	FS ⊥	<100>	<111>	<011>
Temperature Range	253 – 297 K		253 – 297 K		253 – 297 K		
α_1	49.7	49.7	48.9	48.8	50.0	50.2	50.0
α_2	49.6	–	–	48.9	50.3	50.4	50.3
$\bar{\alpha}$	49.65	49.7	48.9	48.85	50.15	50.3	50.15
Total Number of Measurements	n = 3		n = 3		n = 6		
$\bar{\bar{\alpha}} \pm S$	49.67 ± 0.06		48.87 ± 0.06		50.20 ± 0.17		
Temperature Range	297 – 323 K		297 – 323 K		297 – 323 K		
α_1	47.3	46.5	45.3	45.8	47.5	47.6	47.8
α_2	47.0	47.3	46.0	45.5	–	46.6	47.3
$\bar{\alpha}$	47.15	46.9	45.65	45.65	47.5	47.1	47.55
Total Number of Measurements	n = 4		n = 4		n = 5		
$\bar{\bar{\alpha}} \pm S$	47.02 ± 0.38		45.65 ± 0.31		47.36 ± 0.46		

*Refer to symbols key in Table 4.

In the temperature range 297 to 323 K, groups 1 and 3 do not differ significantly at the 90-percent confidence level. The grand average for these five material types is $\alpha = 47.21 \pm 0.44$, n = 9.

Thermal Conductivity (NaI(Tl) at 300 K)

Multiple measurements were made on three oriented single-crystal NaI(Tl) specimens and four Polyscin specimens, and the results are summarized in Table 7.

Table 7
Summary of NaI(Tl) Thermal Conductivity Measurements

Material Description*	Number of Observations	Thermal Conductivity ±S (W/cm K)
IH //	9	$(1.91 \pm 0.37) \times 10^{-2}$
IS ⊥	9	1.77 ± 0.24
FH //	9	1.64 ± 0.21
FS ⊥	9	1.77 ± 0.24
<100>	6	1.77 ± 0.38
<011>	20	1.62 ± 0.31
<111>	10	1.47 ± 0.26

*Refer to symbols key in Table 4.

There is no significant difference between IS⊥, FH//, FS⊥, <100>, and <011> specimens at the 90-percent confidence level. A grand average for these specimens is $\bar{k} = (1.71 \pm 0.28) \times 10^{-2}$ W/cm K, n = 43.

Thermal Shock Resistance (NaI(Tl) at 300 K)

Critical thermal gradient (ΔT_c), as a function of crack length (ℓ), was calculated for plate, bar, and rod specimens of NaI(Tl) tested in light oil and for the condition of infinite heat transfer coefficient using equation 1 (Figure 12). A minimum in the critical temperature gradient occurs at a crack length of about 4.5 mm. The median edge-crack size observed in Polyscin is 2.5 mm. The area above a curve is a region of crack instability, and the area below a curve is a region of stability.

Critical thermal gradient results for oil quenching are shown in Table 8. Comparison of these results with ΔT_c determined from Figure 12 shows generally good agreement of predicted and observed results when the median flaw size is known.

Effects of specimen size were extrapolated by plotting ΔT_c versus surface-area-to-volume ratio for both oil- and air-quenched specimens (Figure 13).

As agreement between observed and calculated ΔT_c was generally good, equation 1 was used to calculate an average heat transfer coefficient in still air, assuming a crack size equal to the median in

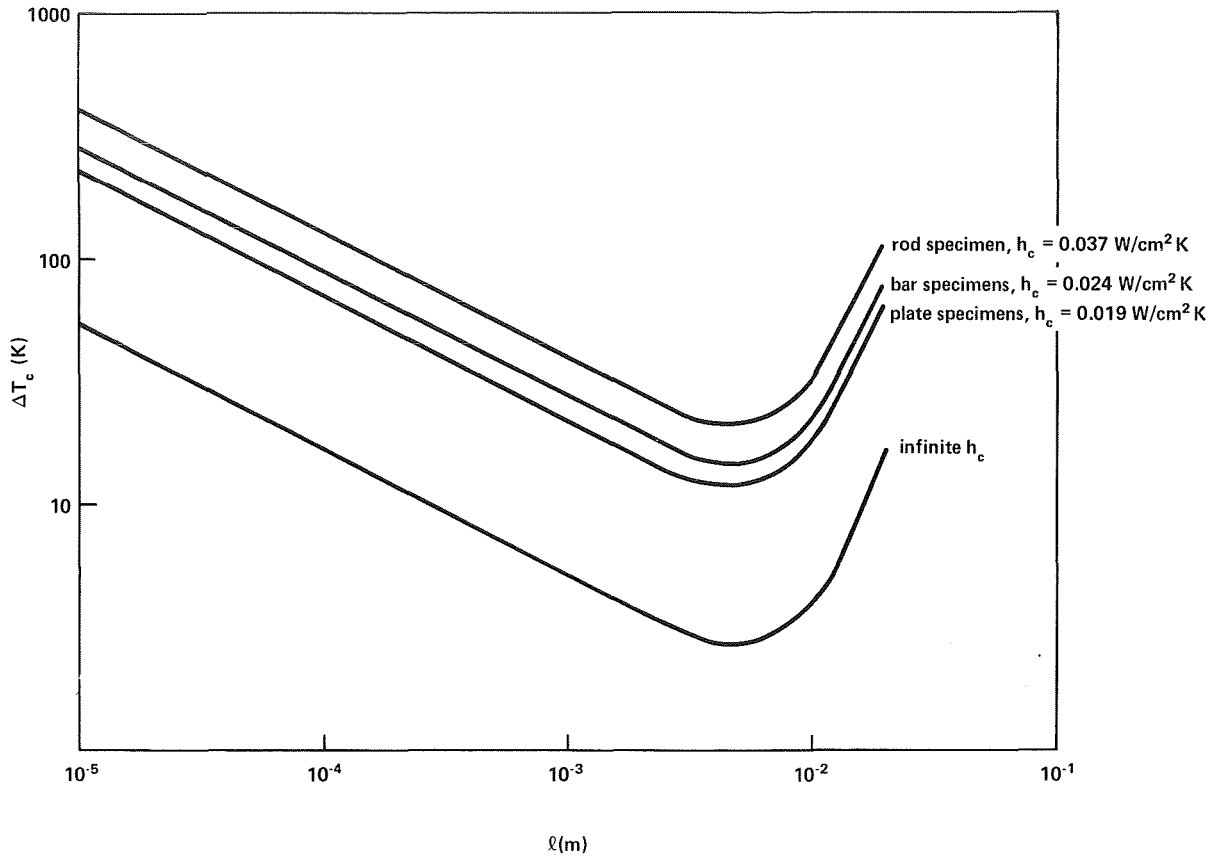

Figure 12. ΔT_c versus ℓ, specimen size, and specimen geometry for NaI(Tl) quenched in light oil.

Table 8
Results of Oil-Quench Testing of NaI(Tl)

Specimen Description	Number of Specimens	ℓ (mm)	Average ΔT_c Observed (K)	Predicted ΔT_c (K)
<100>	3	<0.4	32	35
IH ⊥	3	~2.5	9	14
FS //	3	~2.5	10	14

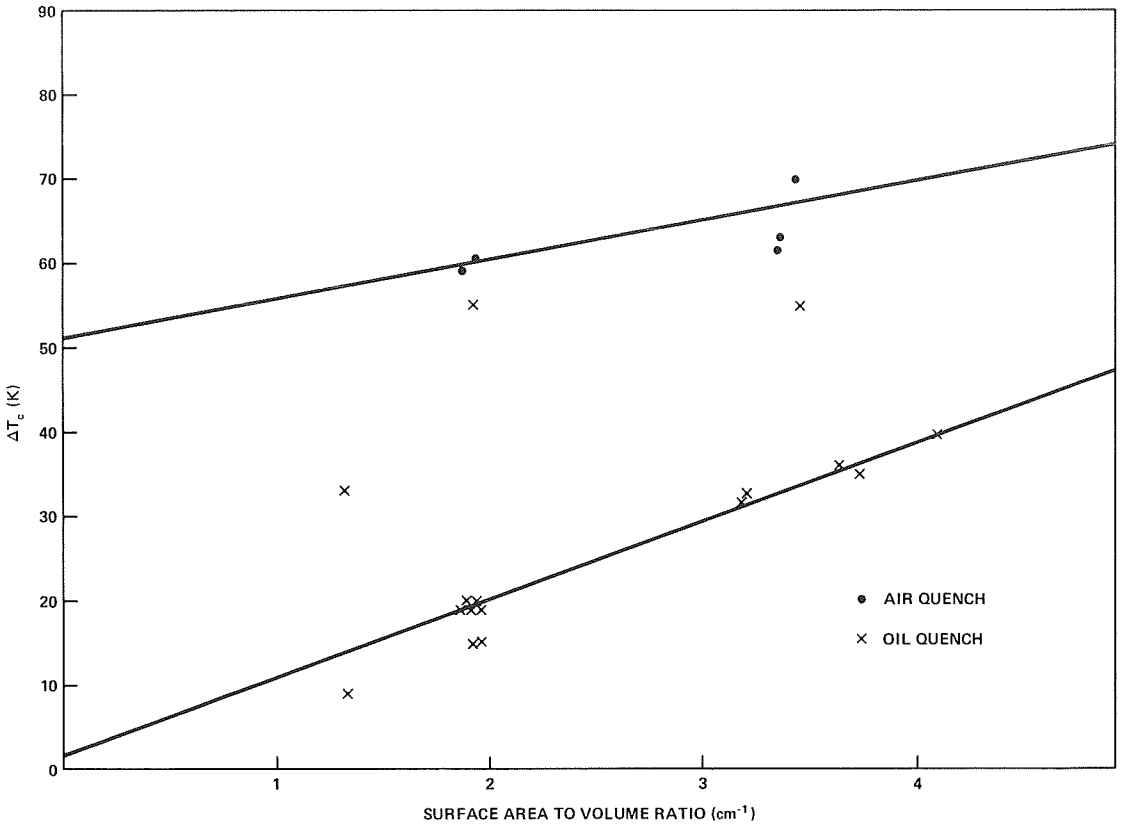

Figure 13. ΔT_c surface-area-to-volume ratio for NaI(Tl) in air- and oil-quench tests.

Polyscin (2.5 mm) and the average ΔT_c observed for rod specimens tested in air (67 K). A value of $h = 1.2 \times 10^{-2}$ W/cm^2 K was calculated.

Heat Capacity (NaI(Tl) at 300 K)

Multiple measurements were made on two single-crystal and two Polyscin specimens, and the results are summarized in Table 9.

Pair-wise hypothesis testing for equality of the means indicates that the means are equal at the 90-percent confidence level. A grand average is $\overline{C}_p = 0.347 \pm 6.61 \times 10^{-3}$ J/gK, n = 28.

Elastic Constants (NaI(Tl) at 300 K)

Results of the density measurements for Polyscin NaI(Tl) are summarized in Table 10.

An F-test for equality of variances fails at the 95-percent confidence level. A t′-test for equality of means indicates that the means are equal at the 95-percent confidence level, giving:

$$\bar{p} = 3.67 \pm 5.61 \times 10^{-3}, n = 35$$

Table 9
Summary of NaI(Tl) Heat Capacity Data

Specimen Number	Specimen Description*	Average Heat Capacity ±S (J/gK)	Number of Observations
1	IH	$0.346 \pm 3.96 \times 10^{-3}$	7
2	FS	$0.350 \pm 1.05 \times 10^{-2}$	7
3	Single crystal	$0.348 \pm 8.66 \times 10^{-3}$	7
4	Single crystal	$0.346 \pm 1.91 \times 10^{-3}$	7

*Refer to symbols key in Table 4.

Table 10
Density of Polyscin NaI(Tl)

Extrusion No.	Average Density ±S (g/cc)	No. of Specimens
1	$3.67 \pm 3.97 \times 10^{-3}$	27
2	$3.66 \pm 9.48 \times 10^{-3}$	8

Results for the measurement of Young's modulus and shear modulus for Polyscin NaI(Tl) are summarized in Table 11.

The mean values for ingot 1, groups 1 through 9, were found to be equal at the 95-percent confidence level, giving an ingot 1 sample size of 34 specimens. The mean values for groups 11 through 14 were found to be equal at the 95-percent confidence level, giving an ingot 2 sample size of 16 specimens. The mean value for these two groups, representing ingot 1 and ingot 2 material, were found to be equal at the 95-percent confidence level, giving a sample size of 50 with the following mean values:

$$E = (2.01508 \pm 0.06258) \times 10^4 \text{ MPa}$$
$$G = (7.64700 \pm 0.28570) \times 10^3 \text{ MPa} \quad , n = 50$$

When tested against the means for specimens measured using the resonance method (group 10), this sample was found to be unequal at the 95-percent confidence level.

The results of elastic-stiffness-constant measurements performed on single crystals of NaI(Tl) are summarized in Table 12.

Table 11
Young's Modulus (E) and Shear Modulus (G) of Polyscin

Group No.	Position Orientation*	Type Specimen†	Number in Sample	E ±S (MPa)	G ±S (MPa)
Extrusion 1, PEO Method (Groups 1-9)					
1	IH //	MOR	4	$(1.9864 \pm 0.0454) \times 10^4$	$(7.5816 \pm 0.4221) \times 10^3$
2	IH ⊥	MOR	4	1.9771 ± 0.0613	7.4867 ± 0.2109
3	IS //	MOR	3	2.0035 ± 0.0227	7.6465 ± 0.1323
4	FH //	MOR	4	1.9821 ± 0.0176	7.5807 ± 0.1115
5	FH ⊥	MOR	3	2.0244 ± 0.0449	7.6685 ± 0.2001
6	FS //	MOR	4	1.9710 ± 0.0305	7.4748 ± 0.0872
7	IH //, IS ⊥ FH //, FS ⊥	TC	4	2.0257 ± 0.0335	7.7102 ± 0.1600
8	FS //	UC	4	1.9589 ± 0.0290	7.3869 ± 0.1153
9	IH ⊥	UC	4	2.0715 ± 0.0240	7.9535 ± 0.0951
Extrusion 1, Resonance Method (Group 10)					
10	IH //, IH ⊥ IS //, FH // FH ⊥, FS //	Q^{-1}	12	$(2.138 \pm 0.072) \times 10^4$	$(8.295 \pm 0.324) \times 10^3$
Extrusion 2, PEO Method (Groups 11-14)					
11	IH ⊥	UC	4	$(2.0359 \pm 0.09112) \times 10^4$	$(7.7461 \pm 0.34966) \times 10^3$
12	FS //	UC	4	1.9693 ± 0.06658	7.4660 ± 0.33760
13	IH ⊥	MOR	4	2.0937 ± 0.04315	7.9012 ± 0.15579
14	FH ⊥	MOR	4	2.0975 ± 0.12773	7.8160 ± 0.48633

*Refer to symbols key in Table 4.

†MOR = modulus of rapture; TC = thermal conductivity; UC = ultimate compression; and Q^{-1} = internal friction.

The mean values for material groups tested by using the PEO method were found to be equal at the 95-percent confidence level, giving a sample of 36 specimens with:

$$C_{11} = (3.0418 \pm 0.0117) \times 10^4 \text{ MPa}$$

$$C_{12} = (8.9581 \pm 0.1035) \times 10^3 \text{ MPa}, \quad , n = 36$$

$$C_{44} = (7.360 \pm 0.0262) \times 10^3 \text{ MPa}$$

Testing the mean of this sample against the mean of specimens measured by using the resonance method indicates that the means are not equal at the 95-percent confidence level. The PEO method is considered to be the most accurate and reliable method.

Table 12
Elastic Stiffness Constants

Ingot No.	Type Specimen	No. in Sample	$C_{11} \pm S$ (MPa)	$C_{12} \pm S$ (MPa)	$C_{44} \pm S$ (MPa)
PEO Method					
1	UC	7	$(3.0283 \pm 0.0049) \times 10^4$	$(8.8579 \pm 0.093) \times 10^3$	$(7.3573 \pm 0.019) \times 10^3$
1	MOR	9	3.0407 ± 0.0137	8.9262 ± 0.1399	7.3573 ± 0.0233
2	UC	6	3.03215 ± 0.0036	8.9427 ± 0.0684	7.3437 ± 0.0044
2	MOR, TC	14	3.0536 ± 0.0133	9.0354 ± 0.0679	7.4017 ± 0.0251
Resonance Method					
1	Q^{-1}	6	$(2.902 \pm 0.099) \times 10^4$	$(8.066 \pm 1.43) \times 10^3$	$(7.323 \pm 0) \times 10^3$

Mechanical damping efficiency (internal friction) was measured by using forced- and free-vibration measurements. Forced-vibration measurements of Q^{-1} were used to assess material effects on Q^{-1}. These measurements reflect Q^{-1} measured at the maximum amplitude attained by the specimen, and these results are shown in Table 13. Free- and forced-vibration measurements for single-crystal material and for Polyscin were averaged to assess the frequency dependence of Q^{-1}, using free-vibration estimates of Q^{-1} of maximum amplitude. These results are shown in Table 14. Finally, strain amplitude dependence of Q^{-1} was observed for many specimens at the flexural, torsional, and longitudinal fundamental frequencies, manifest as a nonlinear decay curve of log amplitude versus time in the free-vibration method. Internal friction was highest at maximum amplitude and dropped to a low limiting value with time as the vibrational amplitude dropped to zero.

Ultimate Strengths

NaI(Tl) at 300 K

Tables 15 and 16 summarize single-crystal bending strengths for NaI(Tl) and Tables 17 and 18 summarize Polyscin bending strengths. All the specimens tested were of the large variety (12.7 by 2.54 by 2.54 cm). Although smaller Polyscin bend specimens (2.5 by 0.6 by 0.3 cm) were also tested, the results for them are summarized in the section on "Susceptibility to Subcritical Crack Growth." Figures 14 and 15 with Tables 19 and 20 give Weibull analyses for Polyscin and single-crystal material, respectively.

Thallium ion concentration measured by atomic absorption using pieces of the fracture surfaces ranged from 416 to 1423 ppm. No correlation of strength to thallium ion concentration was observed.

Tables 21 and 22 summarize single-crystal compressive strength results for NaI(Tl), and Tables 23 and 24 summarize the results for Polyscin.

Table 13
Material Effects on Q^{-1}_{forced} of NaI(Tl) Resonance Specimens
at Fundamental Resonance Frequencies

Material Designation*	No. of Specimens	Flexural F_1 @ 750 Hz	Torsional T_1 @ 2100 Hz	Longitudinal L_1 @ 9500 Hz
<100>	1	5.30×10^{-4}	3.05×10^{-4}	–
<011>	2	2.80×10^{-4}	1.35×10^{-4}	8.66×10^{-5}
<111>	2	3.70×10^{-4}	2.45×10^{-4}	1.63×10^{-5}
Polyscin IH, IS, FS	8	5.12×10^{-4}	2.58×10^{-4}	1.57×10^{-4}
Polyscin FH	4	3.32×10^{-4}		

*Refer to symbols key in Table 4.

Table 14
Internal Friction of NaI(Tl) at Various Frequencies

Vibration Mode and Overtone	Frequency (Hz)	No. of Specimens	Q^{-1} (free)	Q^{-1} (forced)	$Q^{-1} \pm S$
F_1	750	31	$(3.29 \pm 1.9) \times 10^{-4}$	$(4.21 \pm 1.9) \times 10^{-4}$	$(3.74 \pm 1.9) \times 10^{-4}$
F_2	2100	9	$\left(1.08 \begin{smallmatrix}+0.76\\-0.40\end{smallmatrix}\right) \times 10^{-3}$	–	$\left(1.08 \begin{smallmatrix}+0.76\\-0.40\end{smallmatrix}\right) \times 10^{-3}$
F_4	6000–7000	3	$(6.53 \pm 2.0) \times 10^{-3}$	–	$(6.53 \pm 2.0) \times 10^{-3}$
F_6	14000	3	$(2.84 \pm 1.8) \times 10^{-3}$	–	$(2.84 \pm 1.8) \times 10^{-3}$
T_1	2100	32	$(2.82 \pm 1.6) \times 10^{-4}$	$(2.66 \pm 1.7) \times 10^{-4}$	$(2.74 \pm 1.7) \times 10^{-4}$
T_3	6000–7000	6	$\left(6.24 \begin{smallmatrix}+10.5\\-5.2\end{smallmatrix}\right) \times 10^{-4}$	–	$6.24 \begin{smallmatrix}+10.5\\-5.2\end{smallmatrix} \times 10^{-4}$
T_5	11000–12000	3	$(8.36 \pm 1.0) \times 10^{-4}$	–	$(8.36 \pm 1.0) \times 10^{-4}$
L_1	9500	31	$(1.17 \pm 0.4) \times 10^{-4}$	$\left(1.48 \begin{smallmatrix}+1.54\\-0.54\end{smallmatrix}\right) \times 10^{-4}$	$\left(1.32 \begin{smallmatrix}+1.09\\-0.46\end{smallmatrix}\right) \times 10^{-4}$
L_1	15000	3	$(5.11 \pm 1.6) \times 10^{-4}$	–	$(5.11 \pm 1.6) \times 10^{-4}$
L_2	28000	2	$(7.35 \pm 0.9) \times 10^{-4}$	–	$(7.35 \pm 0.9) \times 10^{-4}$
L_3	42000	3	$(4.32 \pm 1.0) \times 10^{-4}$	–	$(4.32 \pm 1.0) \times 10^{-4}$

Table 15
NaI(Tl) Single-Crystal Critical Resolved Tensile Stress in Bending

Ingot No.	Specimen Type*	Average Critical Resolved Tensile Stress ±S (MPa)**	No. Specimens	Group Number
1	<100>	2.38 ± 0.04	3	1
1	<011>	2.36 ± 0.17	3	2
1	<111>	2.32 ± 0.23	3	3
2	<100>	2.50 ± 0.08	3	4
2	<011>	1.85 ± 0.19	3	5
2	<111>	2.27 ± 0.07	3	6
3	<100>	1.65 ± 0.13	3	7
4	<100>	2.58 ± 0.12	4	8
5	<100>	2.45 ± 0.15	4	9
6	<100>	2.32 ± 0.13	4	10
7	<100>	2.16 ± 0.15	4	11
8	<100>	2.52 ± 0.16	4	12
9	<100>	2.06 ± 0.20	4	13

*Refer to symbols key in Table 4.
**Applied stress rate of 0.1956 MPa/s.

Table 16
Results of Pair-Wise t-Testing of Groups 8 Through 13 from Table 15

Group	8	9	10	11	12	13
8	–	†	X	X	†	X
9		–	†	X	†	X
10			–	†	†	X
11				–	X	†
12					–	X
13						–

† signifies arithmetic means are equal at 90-percent confidence level.
X signifies arithmetic means are not equal at 90-percent confidence level.

Table 17
NaI(Tl) Polyscin Modulus of Rupture Results

Extrusion No.	Position Orientation*	No. of Specimens	Average MOR ±S (MPa)**	Group No.
1	IH //	4	3.74 ± 0.66	1
1	IH ⊥	4	4.78 ± 1.85	2
1	IS //	4	3.70 ± 0.41	3
1	FS //	4	3.92 ± 0.43	4
1	FH //	4	5.82 ± 0.95	5
1	FH ⊥	4	5.37 ± 0.78	6
2	IH //	4	5.13 ± 1.47	7
2	FH //	4	5.22 ± 1.11	8

*Refer to symbols key in Table 4.
**Applied stress rate of 0.1956 MPa/s.

Table 18
Results of Pair-Wise t-Testing for Polyscin MOR Data from Table 17

Group	1	2	3	4	5	6	7	8
1	–	†	†	†	X	X	X	X
2		–	†	†	X	X	X	X
3			–	†	X	X	X	X
4				–	X	X	X	X
5					–	†	†	†
6						–	†	†
7							–	†
8								–

† signifies arithmetic means are equal at 95-percent confidence level.
X signifies arithmetic means are not equal at 95-percent confidence level.

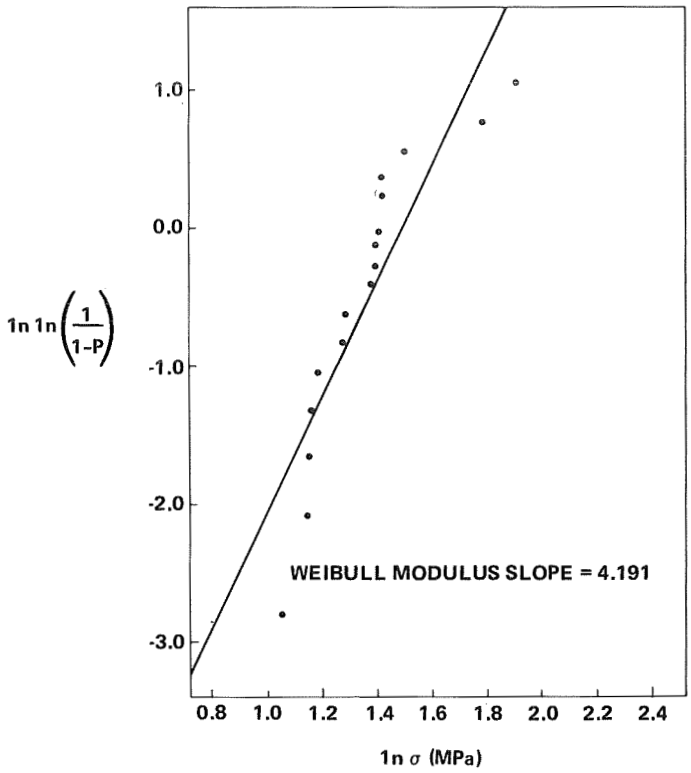

Figure 14. Weibull plot of Polyscin MOR strength data (large specimens).

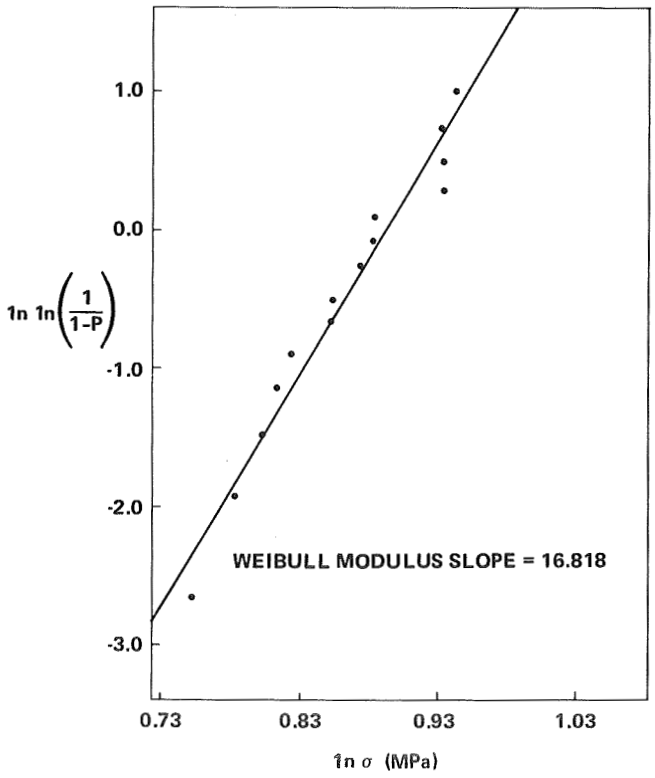

Figure 15. Weibull plot of single-crystal MOR strength data (large specimens).

Table 19
Polyscin Weibull Analysis of Large Specimens*

n	σ_1 (MPa)	ln σ	ln ln (1/1 - P)†
1	2.85	1.049	-2.800
2	3.16	1.150	-2.080
3	3.17	1.154	-1.640
4	3.20	1.162	-1.310
5	3.26	1.182	-1.050
6	3.59	1.281	-0.832
7	3.62	1.286	-0.634
8	4.02	1.391	-0.452
9	4.03	1.395	-0.283
10	4.05	1.398	-0.119
11	4.10	1.411	-0.041
12	4.14	1.420	0.202
13	4.16	1.426	0.369
14	4.52	1.508	0.551
15	5.90	1.775	0.761
16 = N	6.76	1.910	1.040

*12.7 by 2.54 by 2.54 cm.

†P = n/(N + 1).

Table 20
Single-Crystal Weibull Analysis of Large Specimens*

n	σ (MPa)	ln σ	ln ln (1/1 - P)†
1	2.13	0.756	-2.67
2	2.19	0.785	-1.94
3	2.23	0.804	-1.50
4	2.25	0.810	-1.17
5	2.28	0.825	-0.90
6	2.36	0.855	-0.671
7	2.36	0.858	-0.464
8	2.40	0.875	-0.272
9	2.41	0.881	-0.0874
10	2.43	0.887	0.0940
11	2.54	0.934	0.279
12	2.55	0.936	0.476
13	2.55	0.936	0.700
14 = N	2.56	0.942	0.996

*12.7 by 2.54 by 2.54 cm.

†P = n/(N + 1).

Table 21
NaI(Tl) Single-Crystal Compressive Strength

Ingot No.	Orientation Designation*	Average Unresolved Initial Cracking Strength ±S (MPa)	No. of Specimens	Group No.
1	<100>	13.45 ± 2.26	3	1
	<011>	38.51 ± 0.49	3	2
	<111>	50.02 ± 3.63	3	3
2	<100>	13.87 ± 2.48	3	4
	<011>	39.51 ± 0.41	3	5
	<111>	49.73 ± 5.37	3	6

*Refer to symbols key in Table 4.

Table 22
Results of Pair-Wise t-Testing of Groups 1-6 from Table 21

Group	1	2	3	4	5	6
1	–	X	X	†	X	X
2		–	X	X	†	X
3			–	X	X	†
4				–	X	X
5					–	X
6						–

† signifies arithmetic means are equal at 95-percent confidence level.
X signifies arithmetic means are not equal at 95-percent confidence level.

Table 23
NaI(Tl) Polyscin Compressive Strength Data

Extrusion No.	Position Orientation*	Average Initial Cracking Strength ±S (MPa)	No. of Specimens	Group No.
1	FS //	18.88 ± 1.46	4	1
1	IH ⊥	12.45 ± 1.36	4	2
2	FS //	11.38 ± 2.51	4	3
2	IH ⊥	18.02 ± 3.59	4	4

*Refer to symbols key in Table 4.

Table 24
Pair-Wise t-Test Results
of Groups 1-4

Group	1	2	3	4
1	–	X	X	†
2		–	†	X
3			–	X
4				–

† signifies arithmetic means are equal at 95-percent confidence level.
X signifies arithmetic means are not equal at 95-percent confidence level.

Tables 25 and 26 summarize single-crystal and Polyscin shear strength results, respectively.

The NaI(Tl) critical-stress intensity factor was measured by using two methods: the double cantilever beam method and the notched-beam method. Tables 27 and 28 summarize the test results for the double-cantilever-beam method and the notched-beam method, respectively. Using the data from Table 28, Figure 16 is a log plot of the stress intensity equation,

$$K_{IC} = Y \sigma_f \sqrt{a_f}$$

where Y = a geometry constant
σ_f = the stress at failure
a_f = flaw size at failure

CsI(Na) at 300 K

Tables 29 and 30 summarize 0.2-percent compression yield strength results for CsI(Na).

In addition to the single-crystal results, five polycrystalline specimens from ingot 1 had an average yield strength of 2.98 ± 0.22 MPa.

Creep

NaI(Tl) at 300 K

Table 31 and Figures 17 and 18 summarize flexural creep results for Polyscin and single-crystal NaI(Tl) materials. The equation that was fitted to the creep data was:

$$\delta = a + bt^{1/3}$$

Table 25
NaI(Tl) Single-Crystal Shear Strengths

Ingot No.	Orientation*	Average Initial Cracking Stress ±S (MPa)	No. of Specimens
1	<100>	2.16 ± 0.738	2
2	<100>	3.68 ± 3.51	2

*Refer to symbols key in Table 4.

Table 26
NaI(Tl) Polyscin Shear Strengths

Extrusion No.	Position Orientation*	Average Initial Cracking Stress ±S (MPa)	No. of Specimens
1	FS //	3.03 ± 0.45	4
1	IH ⊥	1.79 ± 0.50	4

*Refer to symbols key in Table 4.

Table 27
Double-Cantilever-Beam K_{IC} for NaI(Tl)

Specimen	K_{IC} (MPa $m^{1/2}$)
1	0.43
2	0.31
3	0.52
4	0.58
5	0.33
6	0.54
Average	0.45 ± 0.11

Table 28
Notched-Beam K_{IC} for NaI(Tl)

Specimen	σ_f (MPa)	a_f (cm)	K_{IC} (MPa $m^{1/2}$)
1	4.46	0.571	0.304
2	10.14	0.175	0.384
3	9.22	0.170	0.345
4	9.88	0.173	0.371
5	11.52	0.165	0.423
6	10.58	0.160	0.385
7	7.59	0.378	0.423
8	8.20	0.345	0.463
9	7.91	0.256	0.363
		Average	0.382 ± 0.042

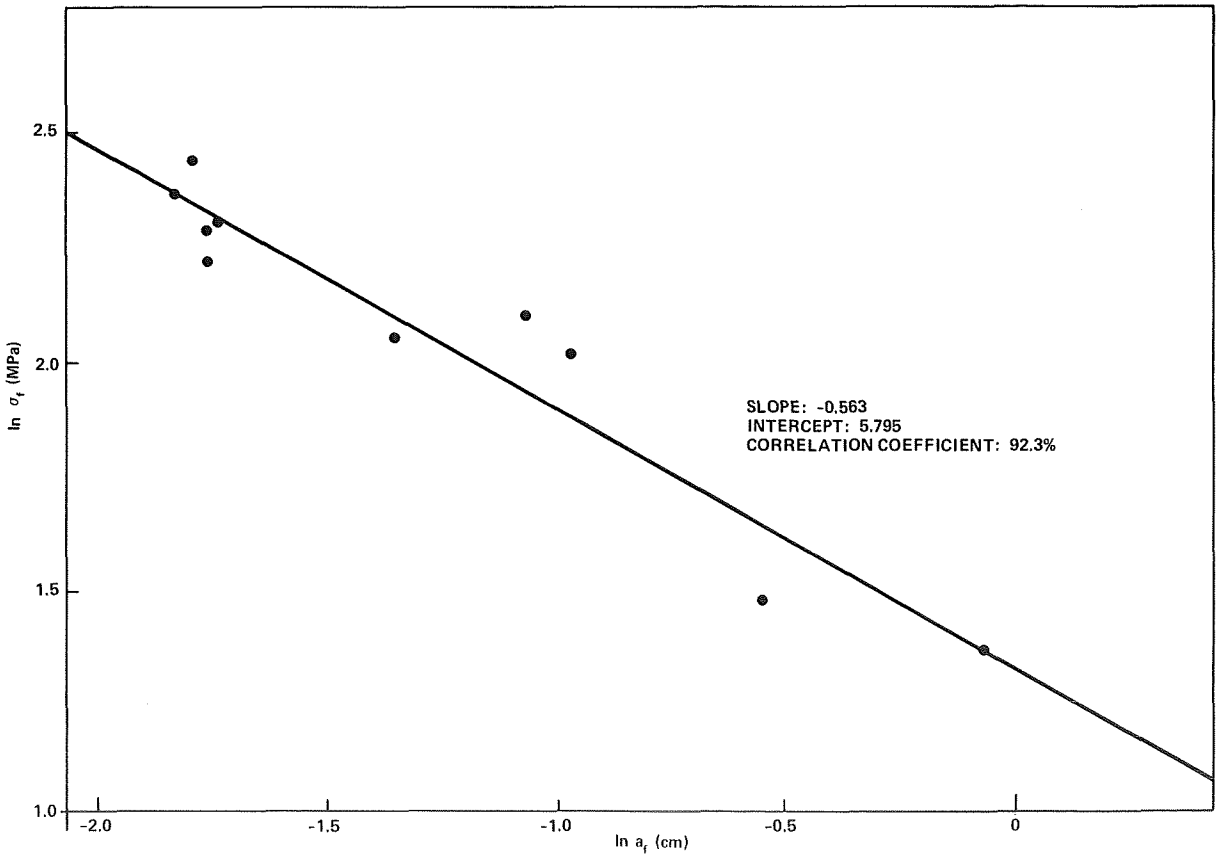

Figure 16. NaI(Tl) K_{IC} notched-beam data.

Table 29
CsI(Na) Single-Crystal 0.2-Percent Compressive Yield Strength (MPa)

Ingot No.	Location*	Orientation*		
		<001>	<011>	<111>
2	T	3.85		
	M	3.27		
	B	3.37	3.89	3.05
	Ave ±S	3.49 ± 0.33		
3	T	5.03		
	M	5.27		
	B	5.02	5.68	2.57
	Ave ±S	5.11 ± 0.14		
4	T	7.49		
	M	7.34		
	B	7.24	6.18	2.84
	Ave ±S	7.36 ± 0.12		

*Refer to symbols key in Table 4.

Table 30
Increase in Average Compressive 0.2-Percent Yield Strength of CsI(Na) with Time

Ingot No.	<100> Compressive Yield Strength (MPa)		Increase (%)
	Tested 2/12/80	Tested 11/18//81	
1*	2.98 ± 0.22	5.45	182
2	3.49 ± 0.33	4.37	125
3	7.36 ± 0.12	15.51	211
4	5.11 ± 0.14	7.34	144

*Five polycrystalline specimens.

Table 31
Summary of NaI(Tl) Flexural Creep Results

Specimen Identification*	Applied Stress (MPa)	Slope ($cm/hr^{1/3}$)	Intercept (cm)	Correlation Coefficient
FS //	3.36	15.32×10^{-6}	79×10^{-6}	0.879
	2.58	4.60	58	0.590
	1.82	No perceptible creep ($<5.08 \times 10^{-5}$ cm/4000 hr)		
IH ⊥	3.42	4.44	66	0.609
	2.61	8.99	48	0.842
	1.85	No perceptible creep ($<5.08 \times 10^{-5}$ cm/4000 hr)		
IH ⊥†	3.75	12.70	5	0.853
	2.93	14.32	15	0.806
	2.19	1.37	23	0.139
<100>	1.48	34.16	190	0.977
	0.765	10.74	66	0.738
<111>	3.32	17.88	84	0.939
<011>	2.59	22.58	35	0.966
<100>	1.86	4.77	89	0.413
<111>†	3.65	22.05	140	0.901
<011>†	2.92	5.43	574	0.442
<100>†	2.19	2.23	13	0.176

*Refer to symbols key in Table 4.
†Second loading after initial creep at lower stresses.

where

δ = midpoint deflection (cm)

t = time (hours)

a = intercept constant in a $t^{1/3}$ plot of δ

b = slope constant in a $t^{1/3}$ plot of δ

Tables 32 and 33 summarize compressive creep results for Polyscin and single-crystal NaI(Tl) material, respectively. The equation that was fitted to the creep data was:

$$\epsilon = a + bt^{1/3}$$

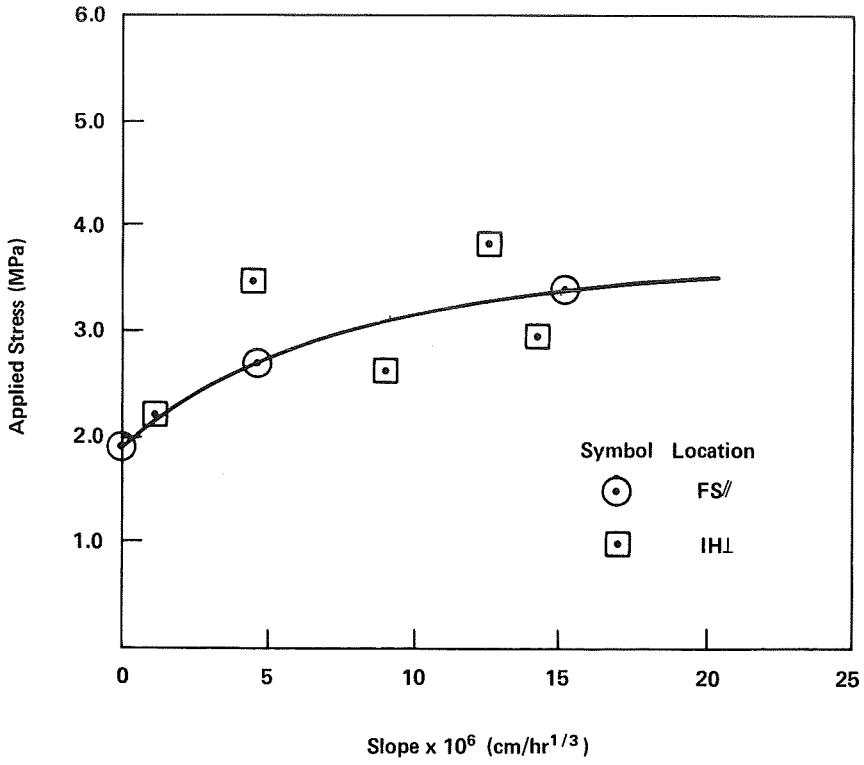

Figure 17. Flexural creep of Polyscin NaI(Tl).

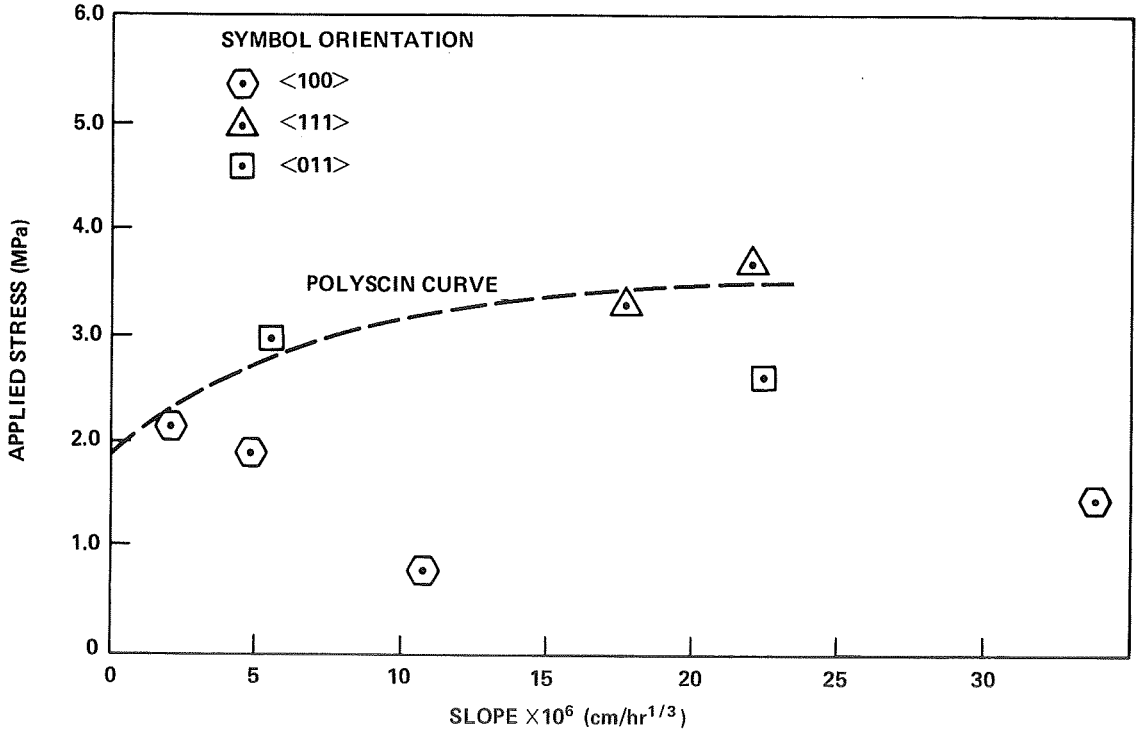

Figure 18. Flexural creep of NaI(Tl) single crystals.

Table 32
Polyscin NaI(Tl) Compressive Creep Summary

Specimen Identification*	Applied Stress (MPa)	Slope (microstrain/$h^{1/3}$)	Intercept (microstrain)	Correlation Coefficient
FS //	1.65	No perceptible creep (<0.005%/2000 hr)		
	2.48	0.62	46	0.184
	4.16	8.19	66	0.844
	6.12	33.83	196	0.963
FS //	1.34	No perceptible creep (<0.005%/2000 hr)		
	2.17†	No perceptible creep (<0.005%/2000 hr)		
	3.82†	No perceptible creep (<0.005%/2000 hr)		
	5.74†	18.55	112	0.973
FS //	1.07	No perceptible creep (<0.005%/2000 hr)		
	1.90†	No perceptible creep (<0.005%/2000 hr)		
	3.55†	9.44	401	0.896
	5.47†	13.34	18	0.859
IH ⊥	1.65	No perceptible creep (<0.005%/2000 hr)		
	2.49†	No perceptible creep (<0.005%/2000 hr)		
	4.18†	1.86	2	0.214
	6.14†	11.61	32	0.706
	7.86†	44.31	242	0.945
IH ⊥	1.37	2.08	-6	0.591
	2.21†	1.16	-12	0.329
	3.89†	6.57	50	0.632
	5.86†	1.00	-15	0.120
	7.40†	5.53	303	0.512
IH ⊥	1.09	1.23	-7	0.673
	1.92†	0.89	1	0.372
	3.60†	2.05	13	0.625
	5.56†	7.47	29	0.941
	7.09†	13.14	118	0.981

*Refer to symbols key in Table 4.
†Progressively increasing stresses applied on the same specimen.

Table 33
Single-Crystal NaI(Tl) Compressive Creep Summary

Specimen Identification*	Applied Stress (MPa)	Slope (microstrain/hr$^{1/3}$)	Intercept (microstrain)	Correlation Coefficient
<111>	1.65	7.01	33	0.917
	2.36†	10.41	32	0.841
	3.48†	18.76	230	0.973
<011>	1.36	No perceptible creep (<0.005%/2000 hr)		
	2.05†	No perceptible creep (<0.005%/2000 hr)		
	3.17†	No perceptible creep (<0.005%/2000 hr)		
<100>	1.08	9.13	34	0.976
	1.78†	No perceptible creep (<0.005%/2000 hr)		
	2.89†	523.6	946	0.9757

*Refer to symbols key in Table 4.
†Progressively increasing stress on the same specimen.

where

ϵ = microstrain

t = time (hours)

a = intercept in a $t^{1/3}$ plot of ϵ

b = slope in a $t^{1/3}$ plot of ϵ

Figure 19 graphically summarizes the Polyscin creep data.

CsI(Na) at 300 K

Table 34 summarizes creep results for polycrystal and single-crystal CsI(Na). The equation that was fitted to the data was:

$$\epsilon = a_1 + a_2 \ln (1 + t/a_3)$$

where

ϵ = microstrain

a_1 = instantaneous creep strain (occurs in <1 minute)

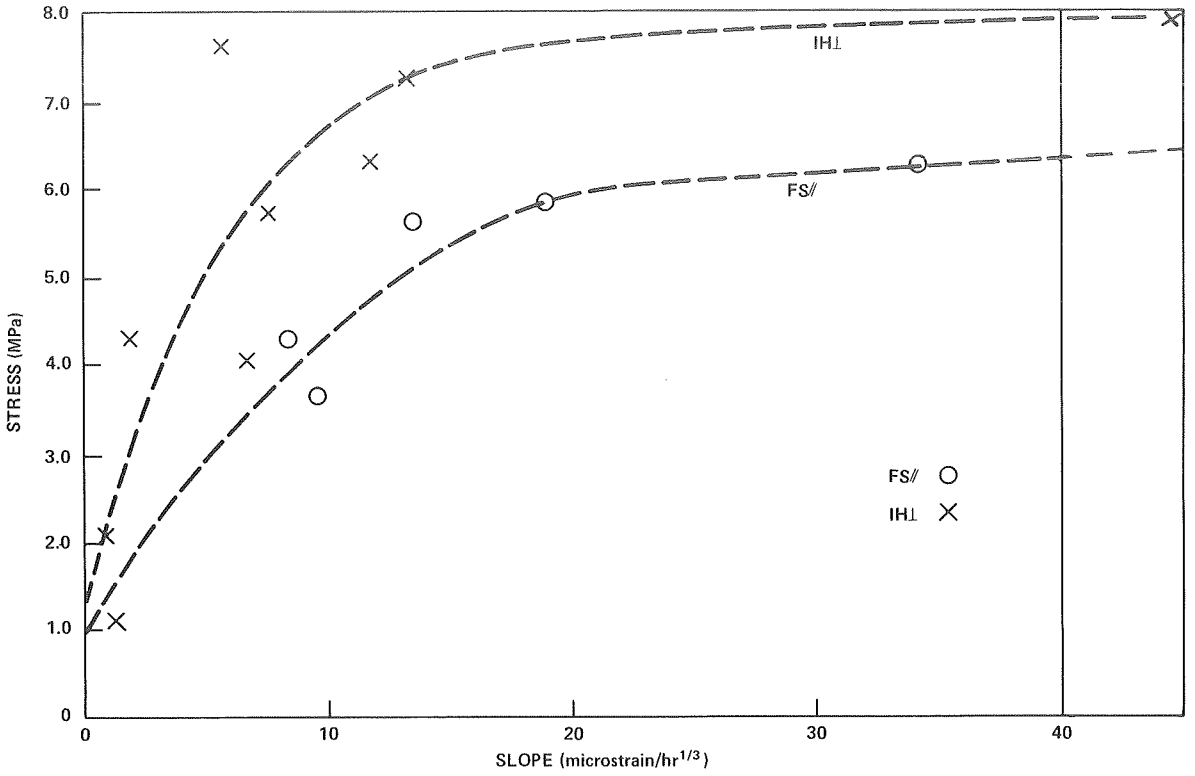

Figure 19. Compressive creep summary for Polyscin.

Table 34
Summary of Constants and Residual Standard Deviations
for CsI(Na) Creep Curves

Ingot No.	Applied Stress (MPa)	Orientation	a_1 (microstrain)	a_2 (microstrain)	a_3	Residuals Standard Deviation
1	2.54	Poly-X	170	1290	8.08 + 00	5.19 - 02
1	4.23	Poly-X	177	7520	4.96 + 01	5.72 - 02
2	2.69	100	1000	92.8	1.21 + 01	1.24 - 02
3	5.99	100	240	64.2	2.62 - 01	6.59 - 03
3	11.00	100	60.4	6.40×10^6	2.10 + 08	1.11 - 03
4	2.07	100	1.15	7.20	7.91 + 00	6.95 - 04
4	4.21	100	68.2	801	3.39 + 03	4.75 - 03
4	7.72	100	641	917	2.58 + 02	1.34 - 02
4	4.49	110	142	2.45×10^7	2.07 + 08	5.37 - 03
4	2.11	111	-85.8	224	1.04 + 00	1.35 - 02

a_2 = a dimensionless fitting parameter (microstrain)

a_3 = a fitting parameter with the dimensions of time (hours)

Hardness (NaI(Tl) at 300 K)

Table 35 summarizes the hardness values for single-crystal NaI(Tl).

Table 35
Vickers Hardness Values for Single-Crystal NaI(Tl)

Measurement Face	Diagonal Direction	Vickers Hardness Number (kg/mm^2)		
		100 g†	300 g†	500 g†
(100)	<100>	9.50	8.62	8.19
(100)	<100>	8.69	7.55	7.74
(111)	$<1\bar{1}0>$	8.69	7.82	8.11
(011)	<100>	8.51	8.01	7.67

†Load.

The mean value for Vickers hardness is 8.12 ± 0.600 kg/mm^2.

Susceptibility to Subcritical Crack Growth (NaI(Tl) at 300 K)

Tables 36 through 39 summarize the results of the stress-rate testing for Polyscin NaI(Tl). Figure 20 and Table 38 give a Weibull analysis of groups 3 and 4 from Table 36.

Ingot Variation

NaI(Tl) at 300 K

In extrusion 1, Polyscin material from the beginning of an extrusion is consistently weaker than material from the end of an extrusion, whereas in the second extrusion, this distinction is not so clear cut. Analysis of the results of the single-crystal NaI(Tl) MOR indicates that each ingot exhibits a characteristic strength with a small standard deviation. On the other hand, Polyscin groups exhibit higher average strength and a rather large standard deviation relative to <100> cleavage strengths. This difference can be explained in terms of the rather small Weibull modulus for Polyscin (~4) relative to the Weibull modulus measured for single-crystal material (~17). Materials with a large Weibull modulus typically exhibit a characteristic strength because of the rather small range in the magnitude of worst flaws. Such materials typically exhibit very little size effect on strength. In contrast, materials with a low Weibull modulus exhibit a large amount of scatter in strength values because of the large range in magnitude of worst flaws. Such materials typically exhibit a significant size effect on strength since the adequate sampling of a flaw population with a large range in the magnitude of worst flaws becomes difficult with small specimens.

Table 36
NaI(Tl) Polyscin Stress-Rate Bend-Test Results

Crosshead Rate (cm/s)	Applied Stress Rate (MPa/s)	No. of Specimens	0.2% Yield Stress ±S (MPa)	Average Flexural Strength ±S (MPa)	Compensated Strength* (MPa)	Group No.
1.69×10^{-5}	0.132	20	5.5 ± 0.9	13.3 ± 0.77	5.56	1
8.47×10^{-5}	0.658	16	6.4 ± 1.2	13.0 ± 0.90	5.44	2
8.47×10^{-4}	6.58	14	–	10.3 ± 0.98	4.31	3
8.47×10^{-3}	65.8	18	6.0 ± 1.3	10.5 ± 0.83	4.39	4

*These specimens were broken in three-point bending with a gauge area of 2.15 by 0.6 cm. Specimens reported in ingot variation testing (Table 17) were broken in four-point bending with an inner and outer span of 3.39 and 10.15 cm, respectively. Because for brittle materials, strength is a function of specimen size and type of loading, it is necessary to make the measurements comparable by using a formula derived from Weibull statistics:

$$\frac{\bar{\sigma}_1}{\bar{\sigma}_2} = \left(\frac{m}{3} + 1\right)^{1/m} \left(\frac{S_2}{S_1}\right)^{1/m} \left(\frac{3m + 6}{4m + 6}\right)$$

where

$\bar{\sigma}_1$ = average strength in three-point loading

$\bar{\sigma}_2$ = average strength in four-point loading

m = Weibull modulus for Polyscin

S_1 = area of a 2.15- by 0.6-cm tensile face of the small three-point bend specimens

S_2 = area of a 10.16- by 2.54-cm tensile face of a hypothetical large three-point bend specimen

The first factor in the above equation converts four-point loading to an equivalent three-point loading. The second factor converts a large specimen tensile surface to a smaller one, and the third factor converts a square cross-section specimen to an equivalent rectangular cross-section specimen (references 26 and 27).

Table 37
Pair-Wise t-Testing Results for
Average Flexural Strengths Listed in
Groups 1-4 from Table 36

Group	1	2	3	4
1	–	†	X	X
2		–	X	X
3			–	†
4				–

† signifies arithmetic mean strengths are equal at 95-percent confidence level.
X signifies arithmetic mean strengths are not equal at 95-percent confidence level.

Table 38
Polyscin Weibull Analysis of Small Specimens*

n	σ (MPa)	ln σ	ln ln (1/1 - P)†
1	5.38	1.683	-3.48
2	6.15	1.817	-2.77
3	6.28	1.837	-2.35
4	6.41	1.858	-2.05
5	6.54	1.878	-1.81
6	7.36	1.996	-1.61
7	7.69	2.040	-1.43
8	8.59	2.151	-1.28
9	8.97	2.194	-1.14
10	9.49	2.250	-1.02
11	9.49	2.250	-0.90
12	9.74	2.276	-0.79
13	9.87	2.290	-0.69
14	10.0	2.303	-0.59
15	10.0	2.303	-0.50
16	10.2	2.322	-0.41
17	10.8	2.380	-0.32
18	10.8	2.380	-0.24
19	10.9	2.389	-0.15
20	11.0	2.398	-0.07
21	11.1	2.407	0.01
22	11.8	2.468	0.09
23	11.9	2.477	0.18
24	12.0	2.485	0.26
25	12.4	2.518	0.35
26	12.8	2.550	0.44
27	12.8	2.550	0.53
28	13.1	2.573	0.64
29	13.6	2.610	0.75
30	14.3	2.660	0.88
31	15.0	2.708	1.03
32 = N	15.7	2.754	1.25

*2.5 by 0.6 by 0.3 cm.
† P = n/(N + 1).

Table 39
Stress-Rate Data for <100> NaI(Tl)
Single-Crystal Impact Specimens*

Fracture Stress (MPa)	Applied Stress Rate (MPa/s)
5.87	1.47×10^4
6.15	1.17
6.55	1.56
6.88	1.71
7.14	1.58
7.37	1.19
7.47	1.13
7.74	1.63
7.96	1.06
8.24	1.73
8.32	1.75
8.36	1.04
8.36	1.67
8.61	1.91
8.69	1.39
9.19	3.68
9.34	1.44
9.43	2.22
10.0	1.25
10.6	3.04
11.7	2.60
11.9	3.96
Average: 8.45 ± 1.61	Average: 1.83×10^4

*6.4 by 0.64 by 0.64 cm.

CsI(Na) at 300 K

CsI(Na) single crystals exhibit extensive ingot variation in 0.2-percent yield strength; however, within an ingot, strength appears to be homogeneous. Creep behavior is also ingot-dependent.

CONCLUSIONS

1. The thallium doping in NaI(Tl) scintillators has little effect on the coefficient of linear thermal expansion, thermal conductivity, heat capacity, and elastic stiffness constants because measured values for these properties on single crystals were equal to values reported in the literature for undoped material.

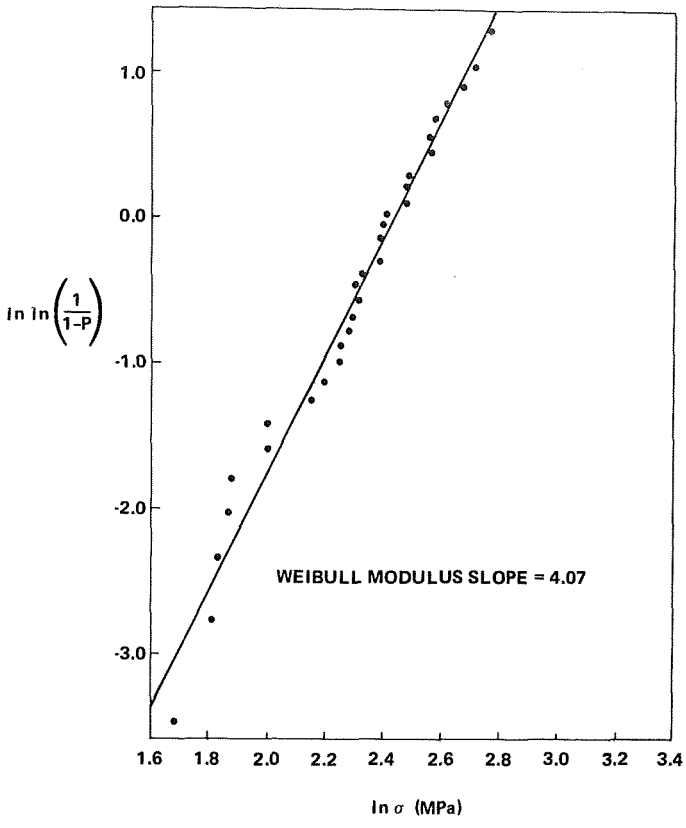

Figure 20. Weibull plot of Polyscin MOR data (small specimens).

2. Strength of single-crystal material is ingot-dependent in both NaI(Tl) and CsI(Na), with CsI(Na) showing the greatest variation. Strength of material within a single-crystal ingot appears to be homogeneous.

3. Strength of Polyscin NaI(Tl) is extrusion-dependent and dependent on position within an extrusion.

4. Strength of Polyscin NaI(Tl) exhibits a significant size effect as predicted by Weibull analysis.

5. The 0.2-percent yield strength of CsI(Na) appears to become greater with time.

6. Creep in both NaI(Tl) and CsI(Na) is ingot-dependent.

7. Although evidence shows that NaI(Tl) does not exhibit subcritical crack growth at stress rates of less than 65.8 MPa/s in less than 3-percent RH room temperature environment, there is some mechanism that more than triples its average strength between stress rates of 65.8 and 1.0×10^4 MPa/s. Possible explanations for this behavior are a susceptibility to

subcritical crack growth at very high stress rates and/or a strength-enhancing brittle transition region between stress rates of 65.8 and 1.0×10^4 MPa/s.

8. No correlation was found to establish a strength dependency on the basis of thallium concentration.

RECOMMENDED TESTING FOR DESIGNERS

Polycrystalline forms of NaI(Tl) and CsI(Na) can be produced by using various forming techniques that utilize temperature and pressure to produce a grain structure in material that is originally a single crystal. Modulus of rupture and compressive creep are considered to be the most diagnostic strength-related measurements for these materials. Creep testing should use a wobble-plate linkage to couple the specimen and the transducers as a means of averaging out errors due to specimens misalignment. These tests, coupled with a K_{IC} measurement and determination of elastic moduli using the pulse-echo overlap technique, should provide a good indication of how these newer materials compare with extruded NaI(Tl) and single-crystal NaI(Tl) and CsI(Na).

ACKNOWLEDGMENTS

This study was initiated by Mr. William Cruickshank who, before his death, contributed greatly to its direction and scope. The authors wish to thank Dr. Robert Hartmann, Mr. Earl Angulo, and Dr. Carl Fichtel of the Goddard Space Flight Center for their assistance in determining materials to be tested and for their continued support. Appreciation is also expressed to Dr. Guy Eubanks and Mr. Walter Viehmann for their guidance and critical analysis. Special thanks are given to Messrs. Ronald Hunkeler, Edward Sanford, and Carl Walch for their technical support in making measurements. Helpful suggestions from Drs. Barrie Hughes and Robert Hofstadter of Stanford University, Dr. James Kurfess of the United States Naval Research Laboratory, and personnel from both the Harshaw Chemical Company and Bicron Corporation are greatfully acknowledged.

REFERENCES

1. Tidd, John L., Joseph R. Dabbs, and Norman Levine, *Scintillator Handbook with Emphasis on Cesium Iodide*, NASA TM X-64741, April 1973.

2. Snyder, R. S., and W. N. Clotfelter, *Physical Property Measurements of Doped Cesium Iodide Crystals*, NASA TM X-64898, August 1974.

3. Hofstadter, R., E. B. Hughes, and B. L. Beron, *Final Project Report on Contract NAS5-20987, Phase B, Definition Study for EGRET Experiment and Hardware*, High Energy Physics Laboratory, W. W. Hansen Laboratory of Physics, Stanford University, Stanford, California, December 1976.

4. *Landolt-Bornstein, Numerical and Functional Relationships in Science and Technology*, New Series K. -H. Hellwege, editor in chief, Group III: Crystal and Solid State Physics, Vol. 1, Elastic, Piezoelectric, Piezooptic and Electrooptic Constants of Crystals, Springer-Verlag, 1966, p. 8.

5. *Thermophysical Properties of Matter*, Vol. 13, Thermal Expansion, Nonmetallic Solids, Touloukian, Kirby, Taylor and Lee. Plenum Publishing Corporation, New York-Washington, 1977.

6. Touloukian, Powell, Ho and Klemens, *Thermophysical Properties of Matter, Vol. 2, Thermal Conductivity*, Nonmetallic Solids, Plenum Publishing Corporation, New York-Washington, 1970.

7. *Handbook of Chemistry and Physics*, 42nd Ed., Chemical Rubber Publishing Company, Cleveland, Ohio, 1960.

8. Touloukian, Y. S., and E. H. Buyco, *Thermophysical Properties of Matter*, Vol. 5, Specific Heat Non Metallic Solids, Plenum Publishing Corporation, New York-Washington, 1970.

9. Poluani, Robert S., Bruce J. Giza, and Christopher S. Tilghman, *Compression Deformation Behavior of CsI(Na)*, Final Technical Report Under Contract S-63970B, Fracture and Deformation Division, National Bureau of Standards, Washington, D.C.

10. Hasselman, D. P. H., "Unified Theory of Thermal Shock Fracture Initiation and Propagation in Brittle Ceramics, *J. Am. Cer. Soc.*, 52(11), 1969, p. 600.

11. Mason, S. S., and R. W. Smith, "Theory of Thermal Shock Resistance of Brittle Materials Based on Weibull's Statistical Theory of Strength," *J. Am. Cer. Soc.*, 38(1), 1955, p. 18.

12. Becker, P. F., et al., Thermal Shock Resistance of Ceramics: Size and Geometry Effects in Quench Tests, *Bull. Am. Cer. Soc.*, 59(5), 1980, p. 542.

13. Emery, A., and A. Kobayashi, "Transient Stress Intensity Factors for Edge and Corner Cracks in Quench Test Specimens," *J. Am. Cer. Soc.*, 63(7-8), 1980, p. 410.

14. Satarmurthy, K., J. P. Singh, D. P. H. Hasselman, "Transient Thermal Stresses in Cylinders with a Square Cross Section Under Conditions of Convective Heat Transfer," *J. Am. Cer. Soc.*, 63(11-12), 1980, p. 694.

15. Chapman, Alan J., *Heat Transfer*, Macmillan Company, New York, 1960.

16. Kreith, F., *Principles of Heat Transfer*, First Ed., In-Text Ed. Publishers, New York, 1973.

17. Mason, Warren P., *Physical Acoustics and Properties of Solids*, D. Von Nostrand Company, Incorporated, Princeton, New Jersey, 1958.

18. Schreiber, Edward, Orson L. Anderson, and Naohiro Soga, *Elastic Constants and Their Measurement*, McGraw-Hill Company, 1973.

19. Krautkramer, J., and H. Krautkramer, *Ultransonic Testing of Materials*, Translation of original edition, Springer-Verlag, New York, Incorporated, 1969.

20. Nowick, A., and B. Berry, *Anelastic Relaxation in Crystalline Solids*, Academic Press, New York and London, 1972.

21. Bradt, R. C., D. P. H. Hasselman, and F. F. Lange, Ed., *Fracture Mechanics of Ceramics*, Vol. 1, Plenum Press, New York-London, 1974.

22. Brown, W. F., and J. E. Srawley, *Plane Strain Crack Toughness Testing of High Strength Metallic Materials*, ASTM Special Technical Publication 410, 1967, pp. 1-13.

23. Nye, J. E., *Physical Properties of Crystals*, Oxford at the Clarendon Press, 1957.

24. Hultquist, Robert A., *Introduction to Statistics*, Holt, Rinehart & Winston, Incorporated, New York, 1969.

25. Wine, R. Lowell, *Statistics for Scientists and Engineers*, Prentice-Hall, Incorporated, Englewood Cliffs, New Jersey.

26. Johnson, C. A., "Fracture Statistics in Design and Application," General Electric Report 79 CRD212, December 1979.

27. Davies, D. G. S., "The Statistical Approach to Engineering Design in Ceramics," *Proc. Br. Ceramic Soc.*, 22, 1973, p. 429.

1. Report No. NASA RP-1131	2. Government Accession No.	3. Recipient's Catalog No.
4. Title and Subtitle Engineering and Design Properties of Thallium-Doped Sodium Iodide and Selected Properties of Sodium-Doped Cesium Iodide		5. Report Date September 1984 6. Performing Organization Code 313
7. Author(s) K. Forrest, C. Haehner, T. Heslin, M. Magida, J. Uber, S. Freiman, G. Hicho, and R. Polvani		8. Performing Organization Report No. 84F0257
9. Performing Organization Name and Address Goddard Space Flight Center Greenbelt, Maryland 20771		10. Work Unit No. 11. Contract or Grant No. 13. Type of Report and Period Covered Reference Publication
12. Sponsoring Agency Name and Address National Aeronautics and Space Administration Washington, D.C. 20546		14. Sponsoring Agency Code

15. Supplementary Notes

K. Forrest, C. Haehner, T. Heslin, M. Magida, and J. Uber: Goddard Space Flight Center, Greenbelt, Maryland.

S. Freiman, G. Hicho, and R. Polvani: National Bureau of Standards, Washington, D.C.

16. Abstract

Mechanical and thermal properties, not available in the literature but necessary to structural design, using thallium-doped sodium iodide and sodium-doped cesium iodide were determined to be coefficient of linear thermal expansion, thermal conductivity, thermal-shock resistance, heat capacity, elastic constants, ultimate strengths, creep, hardness, susceptibility to subcritical crack growth, and ingot variation of strength. These properties were measured for single and polycrystalline materials at room temperature.

17. Key Words (Selected by Author(s))	18. Distribution Statement
Alkali halides, Mechanical properties, Scintillators, Gamma-ray detectors	STAR Category 31 Unclassified—Unlimited

19. Security Classif. (of this report)	20. Security Classif. (of this page)	21. No. of Pages	22. Price*
Unclassified	Unclassified	76	A05

*For sale by the National Technical Information Service, Springfield, Virginia 22161

NASA-Langley, 1984